Parameter and climate data uncertainty as important as climate change for future changes in boreal hydrology

Adrienne M. Marshall[1], Timothy E. Link[2], Gerald Norman Flerchinger[3], and Melissa S Lucash[4]

[1]Georgia Institute of Technology
[2]University of Idaho
[3]USDA - ARS Northwest Watershed Research Center
[4]University of Oregon

November 24, 2022

Abstract

Soil moisture and evapotranspiration (ET) are important components of boreal forest hydrology that affect ecological processes and land-atmosphere feedbacks. Future trends in soil moisture in particular are uncertain, therefore accurate modeling of these fluxes and understanding of concomitant sources of uncertainty are critical. Here, we conduct a global sensitivity analysis, Monte Carlo parameterization, and analysis of parameter uncertainty and its contributions to future soil moisture and ET uncertainty using a physically-based ecohydrologic model in multiple boreal forest types. Soil and plant hydraulic parameters and LAI have the largest effects on summer soil moisture at two contrasting sites. We report best estimates and uncertainty of these parameters via a multi-site Generalized Likelihood Uncertainty Estimation approach. In future scenario simulations, parameter and global climate model (GCM) choice influence projected changes in soil moisture and evapotranspiration as much as the projected effects of climate change in a late-century, high-emissions scenario, though the relative effect of parameters, GCM, and climate vary between objective and study site. Saturated water content, as well as the sensitivity of stomatal conductance to vapor pressure deficit, have the most statistically significant effects on change in evapotranspiration and soil moisture, though there is considerable variability between sites and GCMs. In concert, the results of this study provide estimates of: (1) parameter importance and statistical significance for soil moisture modeling, (2) parameter values for physically-based soil-vegetation-atmosphere transfer models in multiple boreal forest types, and (3) the contributions of uncertainty in these parameters to soil moisture and evapotranspiration uncertainty in future climates.

1   **Parameter and climate data uncertainty as important as climate change for future**

2   **changes in boreal hydrology**

3

4   **Adrienne M. Marshall[1][†], Timothy E. Link[1], Gerald N. Flerchinger[2], Melissa S. Lucash[3]**

5   [1]Department of Forest, Rangeland, and Fire Sciences, University of Idaho, 875 Perimeter Drive, Moscow,

6   ID 83844, USA. [2]USDA Agricultural Research Service Northwest Watershed Research Center, 251 E.

7   Front Street, Suite 400, Boise, ID 83702, USA. [3]Department of Geography, University of Oregon, 1251

8   University Oregon, Eugene, OR 97403, USA

9

10   Corresponding author: Adrienne Marshall (adriennemarshall@gatech.edu)

11   †Current affiliation: School of Civil and Environmental Engineering, Georgia Institute of Technology,

12   790 Atlantic Dr. NW, Atlanta, CA 30332, USA

13

14   **Key Points:**

15   •   Summer soil moisture at rooting depth is most sensitive to soil and plant hydraulic parameters
16   and parameter interactions.

17   •   Parameter uncertainty affects magnitude and sign of projected change in ET and θ_{VWC}; similar
18   effect size to climate change and GCM.

19   •   We present parameter values useful for hydrologic modeling in multiple boreal forest types while
20   recognizing equifinality.

21

Abstract

22

23   Soil moisture and evapotranspiration (ET) are important components of boreal forest hydrology that

24   affect ecological processes and land-atmosphere feedbacks. Future trends in soil moisture in particular are

25   uncertain. Therefore, accurate modeling of these fluxes and understanding of concomitant sources of

26   uncertainty are critical. Here, we conduct a global sensitivity analysis, Monte Carlo parameterization, and

27   analysis of parameter uncertainty and its contributions to future soil moisture and ET uncertainty using a

28   physically-based ecohydrologic model in multiple boreal forest types. Soil and plant hydraulic parameters

29   and LAI have the largest effects on summer soil moisture at two contrasting sites. We report best

30   estimates and uncertainty of these parameters via a multi-site Generalized Likelihood Uncertainty

31   Estimation approach. In future scenario simulations, parameter and global climate model (GCM) choice

32   influence projected changes in soil moisture and evapotranspiration as much as the projected effects of

33   climate change in a late-century, high-emissions scenario, though the relative effect of parameters, GCM,

34   and climate vary between objective and study site. Saturated volumetric water content and sensitivity of

35   stomatal conductance to vapor pressure deficit have the most statistically significant effects on change in

36   evapotranspiration and soil moisture, though there is considerable variability between sites and GCMs. In

37   concert, the results of this study provide estimates of: (1) parameter importance and statistical

38   significance for soil moisture modeling, (2) parameter values for physically-based soil-vegetation-

39   atmosphere transfer models in multiple boreal forest types, and (3) the contributions of uncertainty in

40   these parameters to soil moisture and evapotranspiration uncertainty in future climates.

41

1 Introduction

42

43   Future changes in soil water content (θ_{VWC}) in boreal environments are extremely important and quite

44   uncertain. Soil moisture dynamics interact with water table depths and thaw dynamics to influence

45   growth, wildfire spread (Bartsch et al., 2009), and net ecosystem carbon dynamics in both coniferous

46   (Dunn et al., 2007; Krishnan et al., 2008) and deciduous forest types (Cahoon et al., 2018; Yarie & van

47   Cleve, 2010). θ_{VWC} also influences soil temperature and permafrost degradation via increased soil latent

48   heat of fusion and soil thermal conductivity in wetter soils (Subin et al., 2012). Despite this importance,

49   considerable uncertainty remains: hydrologic models project a wide range of potential future θ_{VWC} in

50   Arctic regions primarily due to differences in moisture partitioning between models (Andresen et al.,

51   2020) and θ_{VWC} has been identified as a crucial missing piece of modeling Arctic and boreal ecosystem

52   dynamics (Fisher et al., 2018). This is perhaps to be expected, given a variety of potential competing

53   mechanisms: for example, permafrost thaw and snowpack decreases could lead to soil drying (Lader et

54 al., 2020; Teufel & Sushama, 2019), while projected increases in rainfall could increase θ_{VWC} (Lader et

55 al., 2017). Changes in evapotranspiration (ET) due to altered vapor pressure deficit also influence θ_{VWC},

56 with potential feedbacks in cases where θ_{VWC} limits ET (Helbig et al., 2020).

57

58 Given these competing mechanisms, process-based hydrologic modeling is an important tool for

59 understanding future changes in boreal soil moisture. However, process-based hydrologic models often

60 suffer from equifinality (Beven, 2006). Sensitivity and uncertainty analyses have emerged as tools to

61 understand and constrain the consequences of equifinality by identifying the parameters to which models

62 are most sensitive and assessing the range of variability in model outputs (Pianosi et al., 2016; Wilby,

63 2005). Global sensitivity analysis methods that explicitly account for interactions between parameters, as

64 opposed to those that rely on modifications of parameters one at a time, are important for

65 comprehensively characterizing model sensitivity (Saltelli et al., 2019). However, these methods can be

66 computationally expensive. The Hilbert-Schmidt Independence Criterion (HSIC) is one approach

67 originating from the machine learning literature that appears to be particularly useful for sensitivity

68 analyses of computationally expensive models with large numbers of parameters (Da Veiga, 2015; Iooss

69 & Lemaître, 2015). Essentially, the HSIC provides an estimate of the dependence of a model outcome on

70 individual input parameters. For estimating model parameter values and associated uncertainty,

71 Generalized Likelihood Uncertainty Estimation (GLUE) methods are a common hydrologic modeling

72 approach favored for their flexibility, relative ease of use, and potential to take advantage of highly

73 parallel computing environments (Beven & Binley, 1992, 2014). GLUE methods require a modeler to

74 specify prior distributions of parameters, generate parameter sets from those distributions, run the model

75 with each parameter set, and identify the parameter sets that result in acceptable model results in

76 comparison with data, which are often deemed "behavioral" in the GLUE parlance.

77

78 Sensitivity and uncertainty analyses have been used to assess the relative contributions of parameter

79 selection, climate model selection, and model structure to hydrologic model outcomes, with varied

80 results. For example, several studies in temperate and mediterranean regions have found that parameter

81 selection is a relatively small source of uncertainty relative to climate input data and hydrologic model

82 structure in streamflow simulations (Chegwidden et al., 2019; Dobler et al., 2012; Feng & Beighley,

83 2020). A study using a monthly water balance model in 61 basins within the Ohio River watershed found

84 that global climate model choice was a more important source of uncertainty for runoff projections, but

85 multi-parameter ensemble uncertainty was more important for soil moisture and groundwater (Her et al.,

86 2019). In another study, uncertainty due to model structure versus climate inputs were of comparable

87 magnitude (Ludwig et al., 2009). In the Colorado River headwaters, choice of calibration data and

88 objective function had a larger effect than choice of hydrologic model on discharge uncertainty (Mendoza

89 et al., 2016). In Arctic regions, Harp et al. (2016) determined that uncertainty in soil hydraulic parameters

90 is a major contributor to future uncertainty in permafrost dynamics, though contributions from climate

91 model uncertainty are even greater. This array of findings suggests that relative importance of different

92 sources of uncertainty depends on geographic context, response variable, model structure, and

93 methodological decisions made by modelers. No such studies to our knowledge have been conducted for

94 soil moisture and ET in boreal regions with discontinuous permafrost.

95

96 In this study, we provide a detailed sensitivity and uncertainty analysis of soil moisture and ET using the

97 Simultaneous Heat and Water (SHAW) model in multiple boreal forest types in order to improve

98 ecohydrologic modeling in this critically important region. Specifically, we (1) identify and rank the

99 sensitivity of modeled soil moisture to SHAW parameters and compare them across forest types, (2)

100 implement an automated calibration procedure to identify parameter values that are transferable across

101 years and forest types, and (3) estimate the effects of calibration-constrained parameter uncertainty on

102 uncertainty of future soil moisture relative to GCM choice and the projected effect of climate change. The

103 results will be useful to those who are interested in understanding and reducing uncertainty in future

104 projections through additional field data collection or focused modeling efforts to improve parameter

105 identifiability. These results will also provide further information about the extent to which efforts to

106 constrain future hydrologic uncertainty should focus on parameter or input data uncertainty, and provide

107 new understanding of how specific parameterization choices affect projections of future conditions.

2 Materials and Methods

108

2.1 Study sites

109

110 In this study, we use data from four previously established field sites that represent two upland birch-

111 dominated sites in different stages of post-fire successional trajectories (US-Rpf and UP1A) and two

112 mature spruce forests underlain by permafrost (Smith Lake 1, 2; Figure 1). These sites were selected

113 based on the diversity of forest structure and ecological conditions, data availability for model forcing and

114 evaluation, and minimization of net lateral hydrologic fluxes by focusing on upland environments (Table

115 1).

116

117 Input climate data sources varied between sites depending on availability. Data for the birch-dominated

118 UP1A was obtained from the Bonanza Creek Long-Term Ecological Research (BNZ LTER) site and

119 described in detail in Marshall et al. (2020). Briefly, collocated hourly air temperature, relative humidity,

120 and wind speed data were obtained and gap filled using correlations with data from nearby weather

121 stations. Downward shortwave radiation was obtained from the US-Uaf AmeriFlux site (Iwata et al.,

122 2010; Ueyama et al., 2009). SHAW corrects shortwave radiation for slope and aspect, minimizing the

123 importance of these differences between sites. Precipitation data was obtained from the LTER1 site, 1 km

124 away from UP1A. US-Rpf is an Ameriflux site dominated by birch with all meteorological variables

125 collected except for winter precipitation. Lacking winter precipitation observations, we used snow depth

126 data from the nearby US-Prr AmeriFlux site and estimated liquid water content of new snow

127 accumulation based on the internal algorithm for newly fallen snow density used in SHAW (Anderson,

128 1976). Soil moisture used for calibration was available at all sites, though depths differed between sites.

129

130 Table 1. Characteristics of the four study sites. Vegetation ages refer to age at the start of the study period.
131 Mean annual temperature (MAT) and mean annual precipitation (MAP) are calculated based on our gap-
132 filled dataset over the years included in the study.

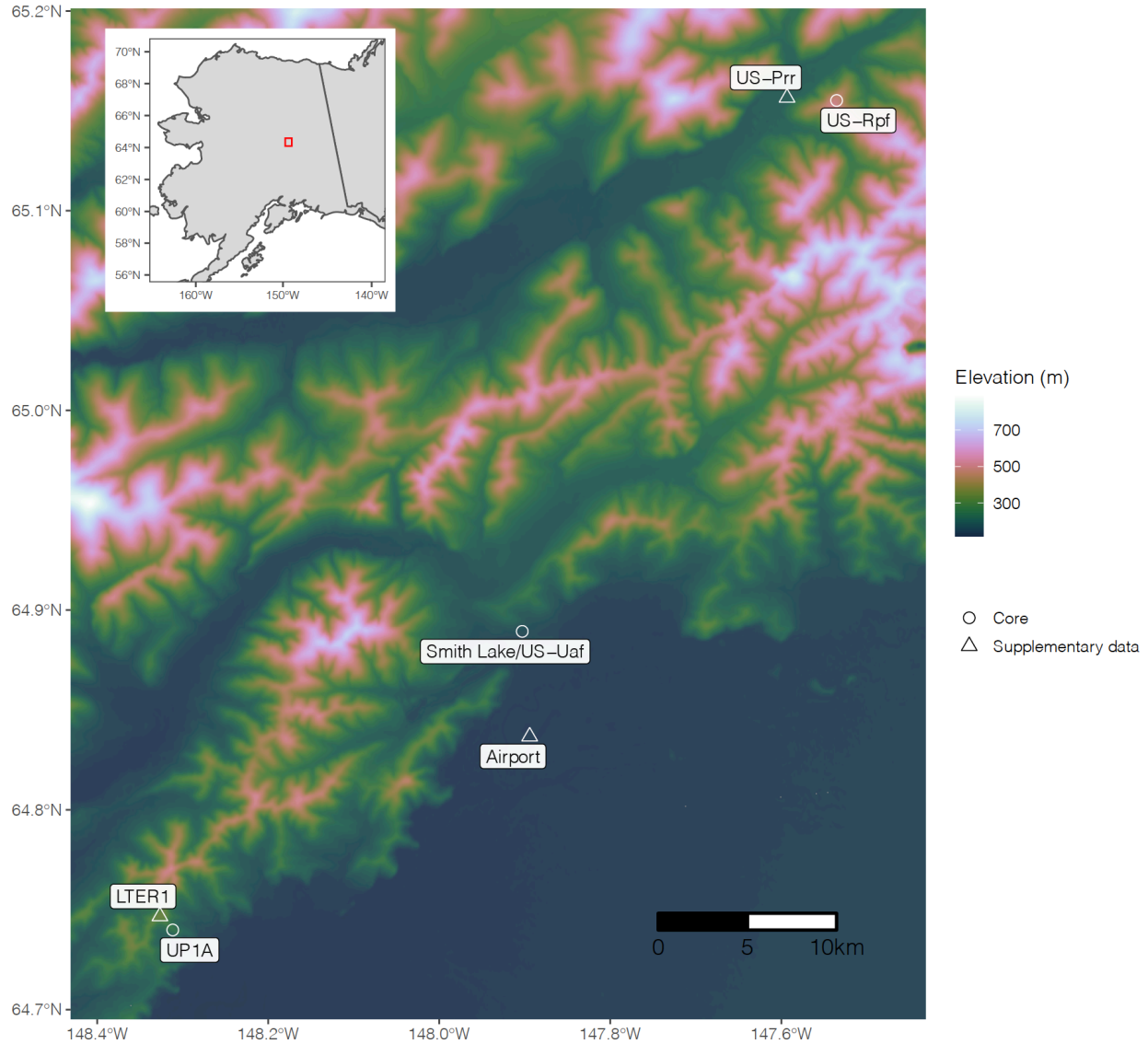| Name	Data source	Years	Vegetation type	Soils	Slope (%)	Aspect	Elevation (m)	Lat, Lon (°)	MAT (°C)	MAP (mm)
UP1A	BNZ LTER	2003-2015	20-year old birch	Silt loam	15	S	258	64.73, -148.30	-1.2	341
US-Rpf	Ameri-Flux	2011-2018	7-year old birch	2 cm organic; sandy loam	15	NE	497	65.12, -147.43	-0.2	453
Smith Lake 1	GIPL; Ameri-Flux	2007-2018	Mature black and white spruce	20 cm organic; silt loam	6	S	160	64.87, -147.86	-2.9	321
Smith Lake 2	GIPL; Ameri-Flux	2007-2018	Mature black spruce	35 cm organic; silt loam	2	N	157	64.87, -147.86	-2.9	321

133

134

135 Figure 1. Study area map, showing core sites for study as well as those used for gap-filling and data

136 supplementation. Red square in the inset shows extent of the larger map.

137

138 The two spruce sites are Smith Lake 1 and Smith Lake 2, both located on the University of Alaska

139 Fairbanks campus and adjacent to the US-Uaf AmeriFlux site. Hourly air temperature, relative humidity,

140 windspeed, and downward shortwave radiation from the AmeriFlux site were used as climate forcings for

141 simulations of both sites. Minimal gap filling was required for air temperature and relative humidity; in

142 each case, one 39-hour period was missing, and data from the previous two days was substituted. In

143 contrast, 27% of the wind data was missing. We filled gaps using a linear interpolation for missing

144 periods less than 6 hours (5% of data), then used a linear regression against colocated wind sensors (at

145   different heights) at the same site for the rest of the missing periods. Daily precipitation data was obtained

146   from the Fairbanks Airport weather station (Menne et al., 2012), which is approximately 5 km to the

147   south. We disaggregated precipitation data to an hourly time step by estimating the number of

148   precipitating hours per day on wet days at the LTER1 weather station (3 hours). We then randomly

149   sampled 3 hours on each wet day and evenly distributed the daily precipitation values over those hours.

150

151   The different sites had varying levels of detail for available vegetation data. Vegetation data for US-Rpf is

152   described in detail in Ueyama et al. (2019), with annual estimates of peak LAI, leaf-on and leaf-off dates,

153   and vegetation height. We estimated biomass for this site based on these data using the allometric

154   equations in Yarie et al. (2007). At UP1A, vegetation surveys provided estimates of stem density and

155   DBH; we estimated biomass and height again following Yarie et al. (2007). The Smith Lake sites have

156   LAI of approximately 2.0 (Iwata et al., 2011) with an 8 m canopy height (Heijmans et al., 2004). Biomass

157   estimates were not available, and were estimated based on relevant literature (Table 2). While this

158   suggests considerable uncertainty in biomass estimates, biomass primarily controls the heat balance of the

159   vegetation layer in SHAW, with minimal effects on hydrology.

160

161   Soil textural data was also obtained from different sources for each site. At UP1A, soil texture was

162   determined based on four soil pits (Yarie, 1998). At US-Rpf, post-burn soils have a 2 cm organic layer,

163   underlain by sandy loams (Ueyama et al., 2019) In the Smith Lake area, organic layer depths were

164   obtained by field observations (*personal communication, Vladimir Romanovsky*), and are underlain by silt

165   loams (NCSS, 2020).

166

167   2.2 SHAW model

168   SHAW is a one-dimensional hydrologic model that simultaneously solves the energy and water balance

169   through the atmosphere-vegetation-snow-soil continuum, with a multi-layer plant canopy, snowpack, and

170   soil profile (Flerchinger, 2017; Flerchinger & Saxton, 1989; Link et al., 2004; Figure 2). SHAW inputs

171   include detailed hourly-to-daily climate data, site characteristics, soil texture and layering, soil and plant

172   hydraulic parameters, and parameters for energy balance-based snow accumulation and ablation (Table

173   2). Outputs include a complete energy and water balance, snowpack dynamics, and soil liquid and frozen

174   water content and temperature at each user-defined node in the soil water profile. The timestep is user-

175   defined, and was hourly in this study. SHAW was initially developed in part to simulate soil moisture

176   dynamics in dynamically freezing soils (Flerchinger et al., 2006; Flerchinger & Saxton, 1989). While this

177   development was based in temperate regions, this feature makes it particularly attractive for modeling in

178 discontinuous permafrost regions. SHAW has previously been applied successfully in boreal and

179 permafrost sites (Marshall et al., 2020; Zhang et al., 2010, 2013).

180

181   2.3 Sensitivity analysis

182 We conducted a global sensitivity analysis of the SHAW model at the burned regenerating birch site and

183 one of the permafrost-underlain spruce sites using the HSIC (Da Veiga, 2015; Iooss & Lemaître, 2015).

184 These two sites were selected to assess sensitivity of soil moisture and evapotranspiration simulations at

185 two contrasting sites. HSIC uses a distance correlation to measure the dependence between an input

186 variable and output variable; it is designed to identify nonlinear dependencies and parameter interactions.

187 Ranges for each parameter were assessed based on literature and available data (Table 2). For a few

188 parameters that are well-defined at each site, such as aspect, the complete possible range was used in

189 order to determine the general importance of these parameters. At each site, 2000 parameter sets were

190 identified using a Latin Hypercube Sampling (LHS) approach with the 'lhs' package in R (Carnell, 2019).

191 The model was run over the calibration period with each parameter set. Average growing season (May-

192 September) soil moisture at the presumed rooting depth for the dominant vegetation at each site (20 cm

193 for black spruce; 60 cm for birch) was calculated for each parameter set. The "sensitivity" package was

194 used to conduct the HSIC sensitivity analysis using universal gaussian kernels and an asymptotic

195 estimation of the p-value (Iooss et al., 2020). When many statistical significance tests are conducted, false

196 discovery rates can be quite high; we followed the method described by Wilks (2016) to identify a p-

197 value that controls the false discovery rate at 10% based on the distribution of p-values obtained from a

198 set of significance tests. This resulted in effective critical p-values of 0.016 at the mature spruce site and
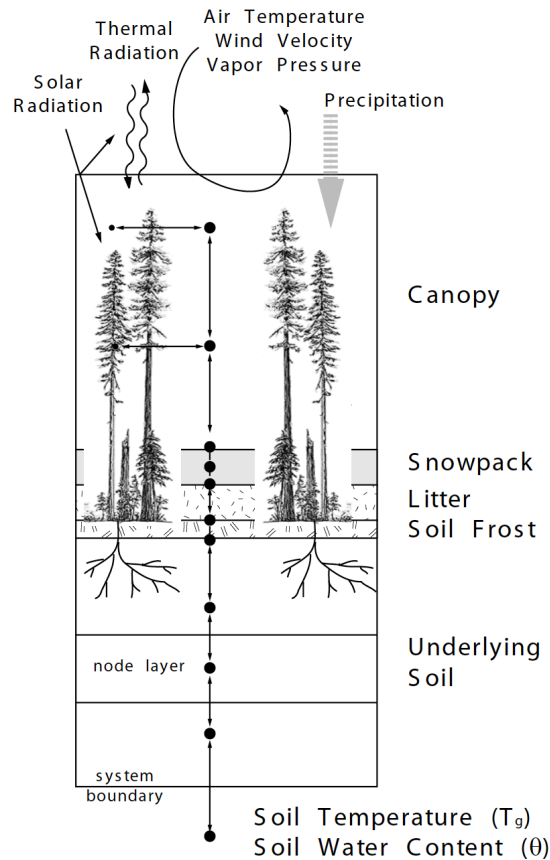
199 0.034 at the burned site.

200

201

202   Figure 2. Conceptual diagram of the SHAW model; originally published in Link et al. (2004). Tree

203   illustrations from Van Pelt (2007). © American Meteorological Society. Used with permission.

204

205   2.4 Multi-site parameter estimation

206   We developed a multi-site framework for estimating regional parameters. Parameters that were

207   determined to be statistically significant in the sensitivity analysis were calibrated using GLUE; the others

208   were estimated based on literature values or known values for the site (Table 2). Results indicated that

209   soil hydraulic parameters were significant in some layers but not others; values for all layers were

210   calibrated for consistency. Parameters that described vegetation water use characteristics, such as

211   minimum stomatal conductance and Jarvis-Stewart environmental feedback parameters, were assumed

212   constant within vegetation types but variable between vegetation types. Organic soil hydraulic parameters

213   were assumed constant between all organic soils in the study. A three-layer mineral soil profile was

214   delineated from 0-20 cm, 20-80 cm, and 80-600 cm. Sites with an organic layer used the organic layer,

215   followed by the second and third mineral layers. Requiring soil hydraulic parameters to remain constant

216   between sites is likely an oversimplification, but lacking a basis on which to systematically vary soil

217 hydraulic parameters within the SHAW framework, this approach was selected to ensure a reasonably

218 simple and consistent parameterization between sites.

219

220 A GLUE methodology was used to calibrate the sensitive model parameters. We used LHS sampling with

221 the parameters that were determined by the sensitivity analysis to significantly affect growing season soil

222 moisture. In order to ensure plausible relationships of parameters between soil layers, specifically K_{sat} and

223 θ_{sat} decreasing with depth and bulk density increasing with depth in mineral soils, we sampled 5×10^6

224 parameter sets, then selected only those that met these criteria, resulting in 22664 parameter sets used in

225 the GLUE method. All parameter sets were run over the first seven years of data available at each site as a

226 calibration period, and daily θ_{VWC} RMSE at the depth with observations closest to presumed rooting depth

227 was evaluated over the May-September growing season. To include evapotranspiration in the parameter

228 selection criteria, we also evaluated the mean absolute error of growing season total evapotranspiration

229 (MAE ET) at the two sites that had observed latent heat fluxes. Results indicated that RMSE of VWC at

230 Smith Lake 2 was particularly poor with all parameter sets, suggesting model structural deficiency at this

231 site as will be discussed later. We therefore did not include ET or VWC from Smith Lake 2 when

232 evaluating the optimal and behavioral parameter sets, in order to avoid introducing objective functions

233 that would select for parameter sets that produce reasonably correct answers for incorrect reasons.

234 Behavioral parameter sets were defined as those with < 0.08 mean RMSE of VWC at the three remaining

235 sites, and < 15% MAE of ET at the site with ET.

236

237   2.5 Climate projections

238 We obtained climate data from the NCAR-CCSM4 and GFDL-CM3 global climate models that were

239 dynamically downscaled using the Weather Research and Forecasting (WRF) model for the years 1970-

240 2100 for the 20 x 20 km grid cells containing each site (Bieniek et al., 2016; Lader et al., 2017). In order

241 to ensure that climate data was relevant to the sites modeled here, we conducted a multivariate quantile

242 mapping bias correction to the gap-filled data for each site (Cannon, 2016). Leaf phenology at both birch-

243 dominated sites was modeled using the relationship between snow disappearance date and leaf-on timing

244 described in Marshall et al. (2020). For each year, we calculated average growing season soil moisture

245 and total growing season ET at the presumed rooting depth at each site with the full set of behavioral

246 parameter sets and evaluated how these trajectories differed between parameter sets. We also used the

247 Hilbert-Schmidt independence criterion to ascertain which parameters contributed most to changes in

248 mean growing season soil moisture in the late-21st century (2070-2099) period relative to a historical

249 (1970-1999) period.

250 Table 2. Parameters used in study. Parameter names indicate variable name used in figures and a description if applicable. The specifier determines whether the

251 parameter was applied to hardwoods (HW) or conifers (Con), and to mineral (M) or organic (O) soil. Case determines whether the parameter was fixed (F) or

252 calibrated (C), based on the sensitivity analysis. Value is the best estimate when fixed, or calibrated value for parameters that are calibrated.

Category	Parameter	Units	Sites	Specifier	Case	Minimum	Value	Maximum	Sources
Plants	clumping		SL2, SL1	Con	F	0.1	0.4	1	Campbell & Norman, 1998
			UP1A, USRpf	HW	F	0.1	0.7	1	
	CriticalLeafWaterPotential (stomatal resistance twice its minimum value)	m	SL2, SL1	Con	F	-236	-174	-112	Dang et al., 1997; Goldstein et al., 1985
			UP1A, USRpf	HW	F	-275	-174	-100	Cable et al., 2014
	CriticalTranspTemp	°C	SL2, SL1	Con	F	-5	0	5	Bonan & Sirois, 1992; Lamhamedi & Bernier, 1994
			UP1A, USRpf	HW	F	-5	0	5	Ranney & Peet, 1994
	DryBiomass	kg/m^2	SL1, SL2	Con	F	0.1	1.7	17	Alexander et al., 2012; Bonan, 1993; Bond-Lamberty et al., 2002.; Melvin et al., 2015; Viereck et al., 1983; John Yarie & Billings, 2002.
			USRpf	HW	F	2.2	2.1	27	Alexander et al., 2012; Bonan, 1993; Melvin et al., 2015; Viereck et al., 1983; Wang et al., 1995; John Yarie & Billings, 2002. Best estimate is allometric.
			UP1A	HW	F	2.2	4.4	27	
	Interception	m/m	SL2, SL1	Con	C	0	1	1	Li et al., 2017; Link et al., 2004
			UP1A, USRpf	HW	C	0	0.76	1	
	K_{St} (influence of solar radiation on stomatal resistance; 0 = no influence)	W/m^2	SL2, SL1	Con	F	0	20.5	100	Bartlett et al., 2003
			UP1A, USRpf	HW	F	0	50	100	Bladon et al., 2006
	K_{vpd} (maximum reduction in stomatal conductance		SL2, SL1	Con	C	0.1	0.14	1	Grossnickle & Blake, 1986

due to vapor pressure deficit)		UP1A, USRpf	HW	C	0.1	0.45	1	Bladon et al., 2006
Leaf area index (LAI)	m²/m²	SL1, SL2	Con	C	0.5	1.9	8	Alexander et al., 2012; Bonan, 1993; Bond-Lamberty et al., 2002.; Chen et al., 1997; H. Iwata et al., 2011; Serbin et al., 2013
		USRpf		C		1.8		Bonan, 1993; Chen et al., 1997
		UP1A		C	0.5	4.5	5.7	
Minimum stomatal resistance ($r_{s,min}$)	s/m	SL2, SL1	Con	C	0.04	1.105	1.174	Bartlett et al., 2003; Cable et al., 2014; Dang et al., 1997; Endalamaw et al., 2017; Körner, 1995; Maire et al., 2015; Salmon et al., 2020
		UP1A, USRpf	HW	C	0.04	0.165	0.178	Blanken et al., 1997; Cable et al., 2014; Dang et al., 1997; Endalamaw et al., 2017; Maire et al., 2015; Murray et al., 2020; Salmon et al., 2020
PlantAlbedo		SL2, SL1	Con	F	0.1	0.3	0.4	Wide range
		UP1A, USRpf	HW	F	0.05	0.3	0.4	Wide range
PlantHeight	m	SL1, SL2	Con	C	1	8.8	10	Alexander et al., 2012; Bonan, 1993; Bond-Lamberty et al., 2002; Heijmans et al., 2004
		USRpf		C	1	1.5	3.8	Alexander et al., 2012; Bonan, 1993; Bond-Lamberty et al., 2002.
		UP1A		C	3	7.8	9.9	
r (coefficient for stomatal conductance due to VPD)		SL2, SL1	Con	C	0.1	0.78	1	Wide range
		UP1A, USRpf	HW	C	0.1	0.11	1	Full possible range
RootingDepth (maximum rooting depth)	m	SL2, SL1	Con	F	0.1	0.2	0.6	Fryer, 2014
		UP1A, USRpf	HW	F	0.1	0.6	1	Safford et al., 1990
StomatalExponent (empirical exponent		SL2, SL1	Con	F	2	5	5	Cable et al., 2014

	relating stomatal resistance to leaf potential)		UP1A, USRpf	HW	F	2	5	5	Flerchinger, 2017
	TempLower	°C	SL2, SL1	Con	F	-5	0	5	Bonan & Sirois, 1992; Lamhamedi & Bernier, 1994
			UP1A, USRpf	HW	F	-5	0	0	Ranney & Peet, 1994
	TempOpt		SL2, SL1	Con	C	11	16.7	25	Bonan & Sirois, 1992; Lamhamedi & Bernier, 1994
			UP1A, USRpf	HW	C	20	21.3	40	Ranney & Peet, 1994
	TempUpper		SL2, SL1	Con	F	32	40	50	Bonan & Sirois, 1992; Lamhamedi & Bernier, 1994
			UP1A, USRpf	HW	F	40	46	50	Ranney & Peet, 1994
	TotalResistance (leaf and root resistance)	m^3s/ton	SL2, SL1	Con	C	50	59	5000	Flerchinger, 2017
			UP1A, USRpf	HW	C	250	467	750	Flerchinger, 2017 with 50% increase and decrease
Residue	DryWeightOfResidue	kg/ ha	SL2, SL1	Con	F	1000	6000	10000	Wide range
			UP1A, USRpf	HW	F	1000	6000	10000	Wide range
	FractionResidue		All		F	0	0.9	0.9	Wide range
	ResidueAlbedo		All		F	0.15	0.25	0.4	Flerchinger, 2017
	ResidueThickness	cm	SL2, SL1	Con	F	0	5	20	Wide range
			UP1A, USRpf	HW	F	1	5	20	Wide range
Site	ponding	cm	All		C	2.5	1.2	10	Wide range
	PrecipThreshold (precipitation falls as snow below this temperature)	°C	All		F	-0.4	1	2.4	Jennings et al., 2018
	roughness (of residue or soil surface)	cm	All		F	0.1	1	10	Campbell & Norman, 1998

Soils	AlbedoDrySoil		All		F	0.1	0.25	0.4	Flerchinger, 2017
	AlbedoExponent (Exponent for albedo of moist soil)		All		F	0.1	0.1	3.5	Flerchinger, 2017
	bulkdensity 1 (ρb 1)	kg/m³	UP1A	M	C	700	913	1720	NCSS, 2020
			USRpf, SL2, SL1	O	C	10	262	300	Liu & Lennartz, 2019
	bulkdensity 2 (ρb 2)		All	M	C	700	1158	1720	NCSS, 2020
	bulkdensity 3 (ρb 3)		All	M	C	700	1223	1720	NCSS, 2020
	ksat 1 (saturated hydraulic conductivity)	cm/hr	UP1A	M	C	0.027	234	270	Blain & Milly, 1991; Chappell et al., 1998; Grayson et al., 1992; NCSS; 2020
			USRpf, SL2, SL1	O	C	0.0017	443	1148	Liu & Lennartz, 2019
	ksat 2		All	M	C	0.027	181	270	Blain & Milly, 1991; Chappell et al., 1998; Grayson et al., 1992; NCSS, 2020
	ksat 3		All	M	C	0.027	141	270	Blain & Milly, 1991; Chappell et al., 1998; Grayson et al., 1992; NCSS, 2020
	lowerBC (soil temperature at lower boundary)	°C	USRpf		F	0	2.4	5	Soil temperature observations
			SL2		F	-5.1	-1.1	2.9	Soil temperature observations
			SL1		F	-4.4	-0.4	3.6	Soil temperature observations
			UP1A		F	0	0.5	5	Soil temperature observations
	poreconn 1 (τ 1; van Genuchten pore connectivity)		USRpf, SL2, SL1	O	C	-5.22	-1.66	1.06	Liu & Lennartz, 2019
	residual volumetric water content 1 (θres 1)		UP1A	M	C	0.017	0.021	0.14	NCSS, 2020
			USRpf, SL2, SL1	O	C	0.004	0.149	0.2	Liu & Lennartz, 2019

θres 2		All	M	C	0.017	0.071	0.14	NCSS, 2020
θres 3		All	M	C	0.017	0.088	0.14	NCSS, 2020
θsat 1		UP1A	M	C	0.34	0.566	0.59	NCSS, 2020
		USRpf, SL2, SL1	O	C	0.62	0.625	0.99	Liu & Lennartz, 2019
θsat 2		All	M	C	0.34	0.546	0.59	NCSS, 2020
θsat 3		All	M	C	0.34	0.454	0.59	NCSS, 2020
van Genuchten alpha (vG α 1)	m^{-1}	UP1A	M	C	0.65	4.44	5.1	NCSS, 2020
		USRpf, SL2, SL1	O	C	1	30.2	45	Liu & Lennartz, 2019; limited upper range because model failed above ~45
vgAlpha_2 (van Genuchten alpha) (vG α 2)		All	M	C	0.65	2.3	5.1	NCSS, 2020
vgAlpha_3 (van Genuchten alpha) (vG α 3)		All	M	C	0.65	4.77	5.1	NCSS, 2020
vgn_1 (van Genuchten n) (vG n 1)		USRpf, SL2, SL1	O	C	1.29	1.54	1.6	Dettmann et al., 2014; Zhang et al., 2010

253

254

255 **3 Results**

256   3.1 Parameter sensitivity

257   At the permafrost-underlain Smith Lake site, growing season θ_{VWC} at the assumed maximum rooting

258   depth (20 cm) was most sensitive to soil hydraulic parameters in the depth at which soil moisture was

259   assessed (layer 1), as well as parameters that control plant water use, including minimum stomatal

260   resistance ($r_{s,min}$), LAI, the Jarvis-Stewart r parameter that controls the influence of vapor pressure deficit

261   on stomatal resistance, and total resistance in leaves and roots (Figure 3). Growing season θ_{VWC} was also

262   sensitive to K_{sat} in the second layer and van Genuchten α in the third layer, as well as maximum canopy

263   interception depth per LAI and aspect. Results at the US-Rpf site were similar. The top four parameters

264   with the largest influence on growing season θ_{VWC} at 60 cm were soil hydraulic parameters in the layer at

265   which soil moisture was evaluated; soil hydraulic parameters for the other layers, particularly α, k_{sat}, and

266   θ_{res} were also important in the sub- and superjacent layers. As at Smith Lake, $r_{s,min}$ and r were significant.

267   Notably, peak LAI at this site was not statistically significant, while a few additional controls on plant

268   hydraulics were: optimum transpiration temperature, plant height, and K_{vpd} were all statistically

269   significant. Moreover, slope and maximum ponding depth, in addition to aspect, were significant at this

270   site.

271

272   To assess the sign of the parameter effects, we compared parameter distributions for the wettest and driest

273   simulations at each site (Figure 4). Distributions that are very dissimilar between the wettest and driest

274   simulations indicate that a parameter has a strong and consistent effect, while those with large overlap

275   indicate either weaker effects or that parameter interactions are more important than the parameter value

276   itself. Many of these are to be expected based on a priori knowledge of the physics represented in the

277   SHAW model: for example, high LAI, low $r_{s, min}$, and south-facing aspects reliably result in drier soils.

278   Similarly, in the layer at which growing season θ_{VWC} was evaluated at each site, low θ_{res}, low θ_{sat}, and

279   higher α tend to result in drier θ_{VWC}. Less obvious are the contrasting effects of soil hydraulic parameters

280   in sub- and superjacent layers: for example, at the US-Rpf site, high θ_{res} in the third layer tends to yield

281   drier θ_{VWC} in the second layer. While this is also a natural consequence of the physics represented in the

282   model, it may be less obvious to modelers conducting manual parameterizations. Finally, some

283   parameters, such as plant height and maximum interception, have a statistically significant effect on

284   growing season θ_{VWC} but limited discernable difference in their distributions between the driest and

285   wettest 1% of cases. This may suggest that the HSIC metric is identifying parameters with a relatively

286   small effect size, or that there are complex parameter interactions that minimize the relationship between

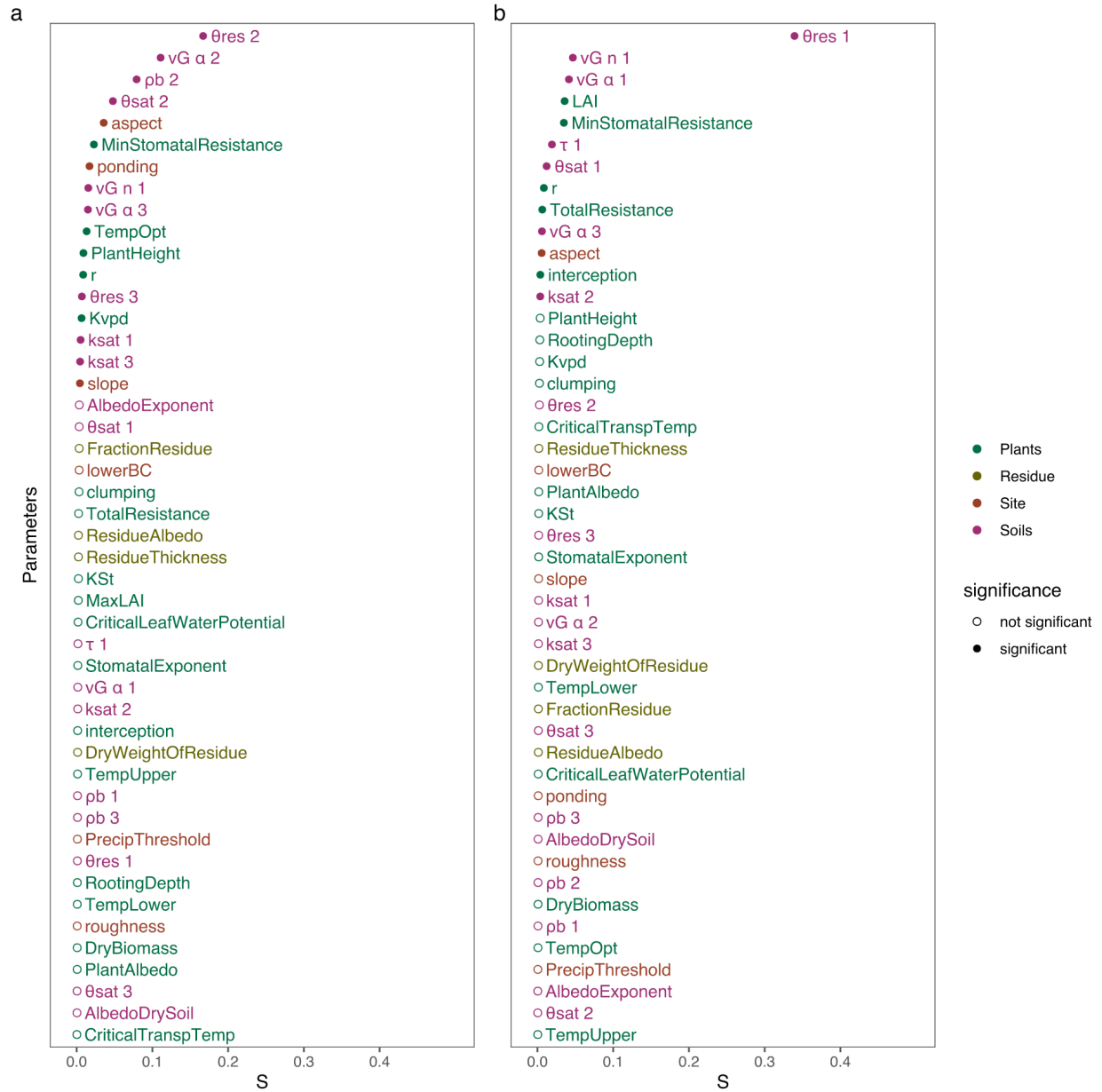287   an individual parameter and θ_{VWC}.

288

289

Figure 3. Results of sensitivity analysis at (a) US-Rpf and (b) Smith Lake 2. Significance threshold was $p < 0.034$ at US-Rpf and $p < 0.016$ at Smith Lake 2. S is the Hilbert-Schmidt Independence Criterion.
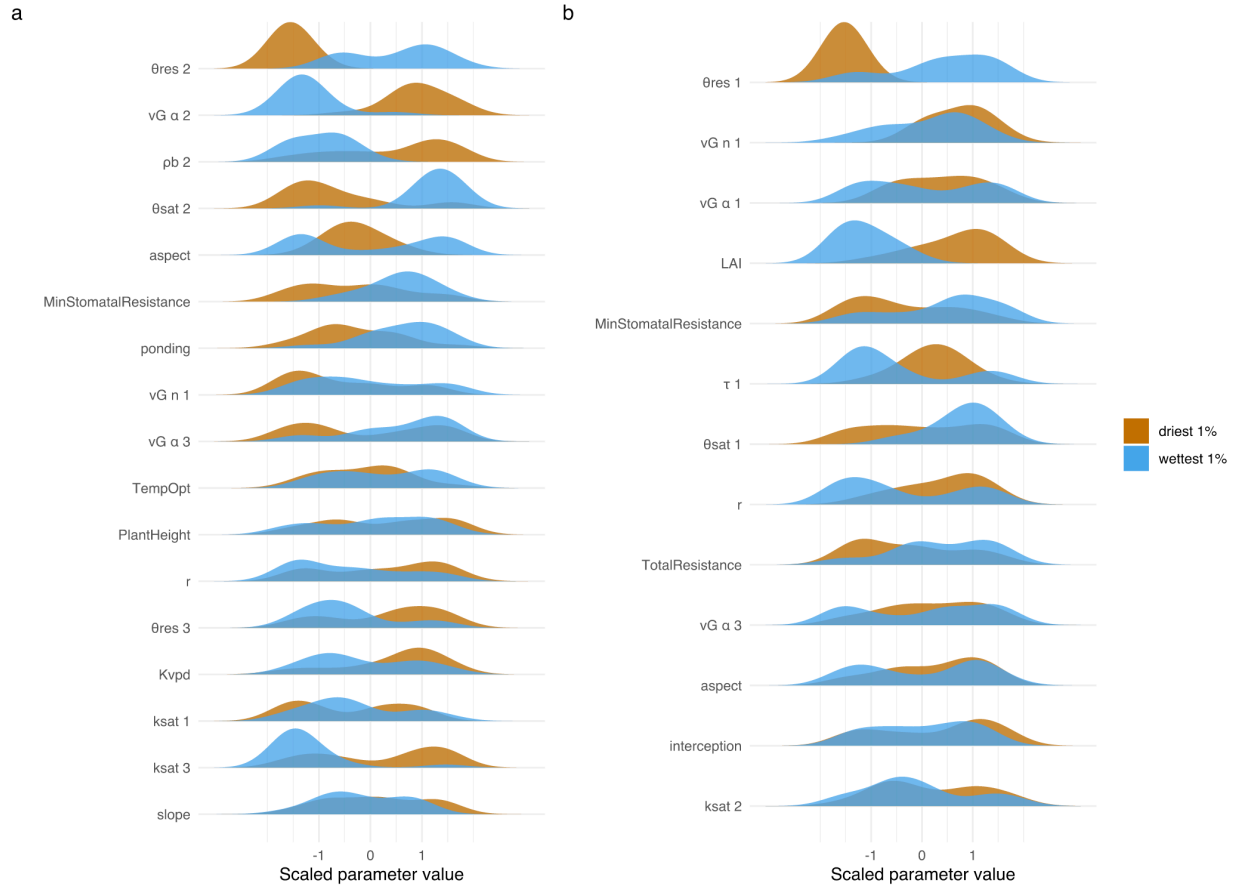
292

293

294   Figure 4. Distribution of the statistically significant parameter values for the driest and wettest 1% of runs

295   at (a) US-Rpf and (b) Smith Lake 2. Parameter abbreviations are detailed in Table 2.

296

297   3.2 GLUE results

298   In the GLUE analysis, 40% of 22,664 parameter sets completed the model runs at all four sites, with some

299   differences between sites: 99.8% finished at UP1A; 77.0% finished at Smith Lake 2; 69.5% finished at

300   Smith Lake 1; and 61.2% finished at US-Rpf. Runs that do not complete are likely due to unrealistic

301   parameter combinations that cause numerical instabilities in the finite difference solutions employed in

302   the SHAW model. The minimum θ_{VWC} RMSE between sites suggests some discrepancy between

303   performance at each site: at Smith Lake 1 and 2, the minimum RMSEs were 0.087 and 0.111,

304   respectively, while these values were 0.026 and 0.030 at UP1A and US-Rpf. Minimum MAE of ET was

305   3.3% and 9.6% at Smith Lake 2 and US Rpf, respectively. After Smith Lake 2 results were discarded due

306   to poor simulation of soil moisture, 45% of parameter sets completed the model run at the three remaining

307   sites. Correlations between objective functions suggested some tradeoffs and synergies: for example,

308   θ_{VWC} RMSE at US-Rpf was positively correlated with that at Smith Lake 1 (Pearson's $r = 0.5$), while

309 RMSE of VWC at UP1A was negatively correlated with θ_{VWC} RMSE at both US-Rpf and Smith Lake 1,

310 indicating that there are tradeoffs in parameter selection between UP1A and the other two sites. MAE of

311 ET was positively correlated with θ_{VWC} RMSE at US-Rpf ($r = 0.3$), implying that parameter sets that

312 modeled ET well tended to also model θ_{VWC} well.

313

314 The criteria for behavioral parameter sets, with MAE ET at US-Rpf less than 15% and mean θ_{VWC} RMSE

315 across three sites < 0.08, resulted in 27 parameter sets. The distributions of behavioral parameter sets

316 suggested that some, but not all of the parameters were better constrained post calibration (Figure 5), as

317 indicated by less variable (e.g. LAI at UP1A) as opposed to similar (e.g.: θ_{sat} 2M) posterior parameter

318 distributions. Note that in some cases, a uniform prior distribution was not used, due to our restrictions on

319 the changes in some soil hydraulic parameters with depth. In behavioral parameter sets, bulk density of

320 the organic layer tended to be high relative to the prior distribution. LAI was at the low end of the

321 distribution at the US-Rpf site, and higher at the UP1A site. $r_{s,min}$ was generally higher in the posterior

322 than prior distribution. The van Genuchten pore connectivity term, τ, in the organic layer was generally in

323 the higher range of the prior distribution, and van Genuchten α was relatively high in the organic layer,

324 but low in the first and second mineral soil layers. Parameter values based on individual sites or objective

325 functions were quite different from each other in many cases, illustrating the importance of calibration on

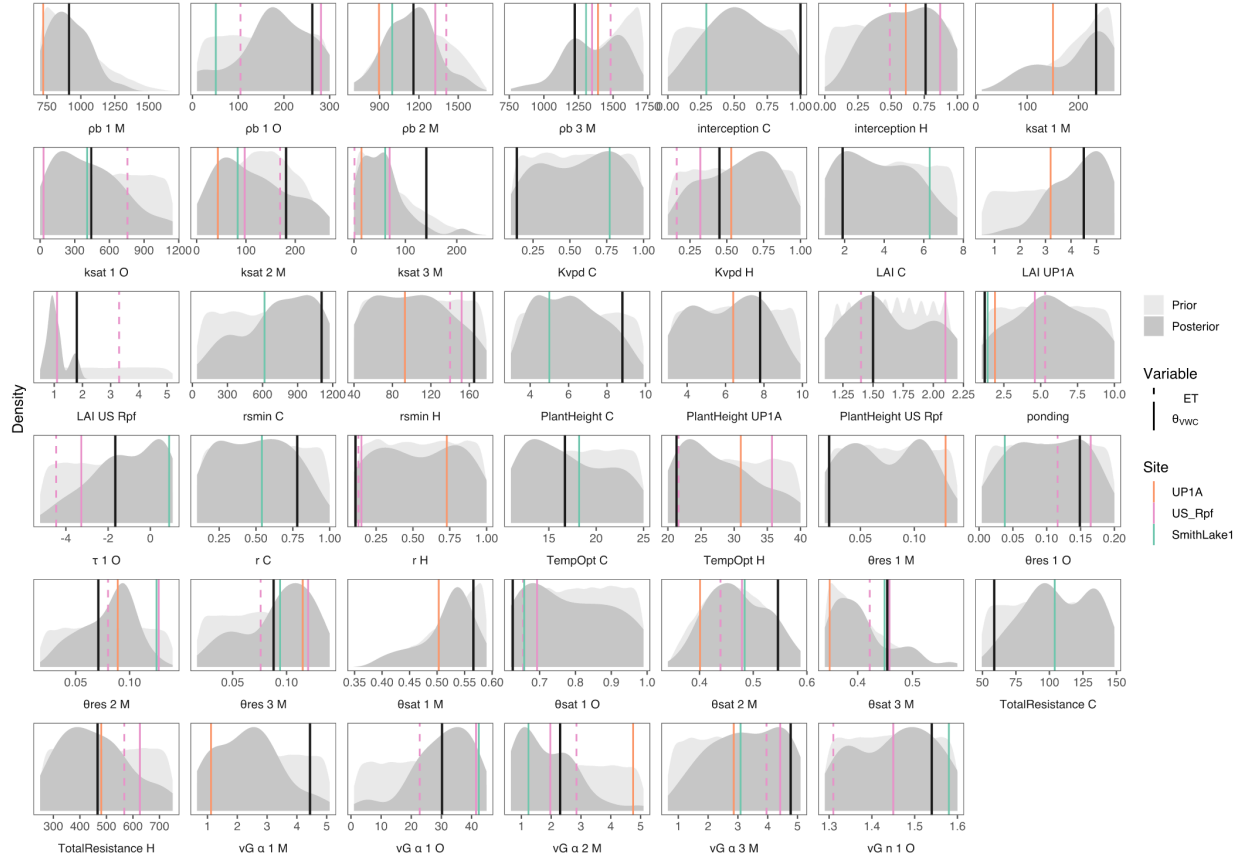326 multiple sites and hydrologic variables when possible.

327

Figure 5. Distribution of behavioral parameter sets. Vertical lines for each site (colors) and variable used in the objective function (line type) indicate the parameter values in the optimal parameter set for each site and variable. The black vertical lines indicate the best overall parameter. Parameter abbreviations are detailed in Table 2.

The optimal parameter set based on multiple objective functions resulted in θ_{VWC} RMSE of 0.10 at Smith Lake 1, 0.05 at UP1A, and 0.08 at US-Rpf, with MAE ET at US-Rpf equal to 9.0%. This parameter set had considerably higher interception per LAI, K_{vpd} in conifers, and LAI in conifers and at UP1A than the best prior estimates. The best estimate of $r_{s,min}$ was slightly higher in conifers and lower in hardwoods than the best prior estimate. Optimum temperatures for transpiration were quite close to the best prior estimate. The best estimated maximum ponding depth was at the very high end of the potential range. K_{sat} was much higher in mineral layers and lower in the organic layer than the best prior estimate; this may reflect in part the fact that values for mineral layers were obtained directly from a lab-based database, while values for organic layers were obtained from literature with values presented over many orders of magnitude. τ, which is often set to 0.5 in mineral soils but may be much lower in organic horizons (Dettmann et al., 2014), was much higher than the best estimate for organic soils, and close to the typical

345   value in mineral soils. van Genuchten α was considerably larger in both the mineral and organic layers

346   than best prior estimates.

347

348   3.3 Reproduction of soil moisture and ET

349   SHAW generally reproduced temporal soil moisture patterns well, but the multi-site solution represented

350   tradeoffs for individual sites (Figure 6). For example, the parameter set that minimized θ_{VWC} RMSE at US

351   Rpf resulted in θ_{VWC} that was consistently too high at UP1A, and too low at Smith Lake 1. Parameter sets

352   that performed well at three sites performed extremely poorly at Smith Lake 2, and in many cases model

353   convergence issues prevented the runs from completing at that site. In addition to the overall poor

354   performance at Smith Lake 2, this reinforces the finding that model structural deficiency likely limits

355   model performance at this site. The multisite compromise tended to be somewhat too dry in the summers

356   at Smith Lake 1 and too wet in the winters at US-Rpf, but captured soil moisture dynamics at UP1A very

357   well.

358

359   Comparisons of modeled and observed ET at US-Rpf indicate that the behavioral parameter sets generally

360   contained observed summer ET and consistently underestimated winter ET (Figure 7). The best parameter

361   set and the set based on minimizing MAE ET tended to overestimate summer ET. In contrast, the set that

362   was selected to minimize the θ_{VWC} RMSE at US-Rpf tended to underestimate ET. Model performance

363   generally declined slightly from the calibration to validation period with respect to θ_{VWC} RMSE. In the

364   multisite compromise, θ_{VWC} RMSE increased from 0.112 to 0.123 at Smith Lake 1 (+0.011), from 0.072

365   to 0.079 at UP1A (+ 0.007), and from 0.054 to 0.072 at US-Rpf (+0.017). The MAE of ET actually

366   decreased from the calibration to validation period, from 18% to 14% (-4%).
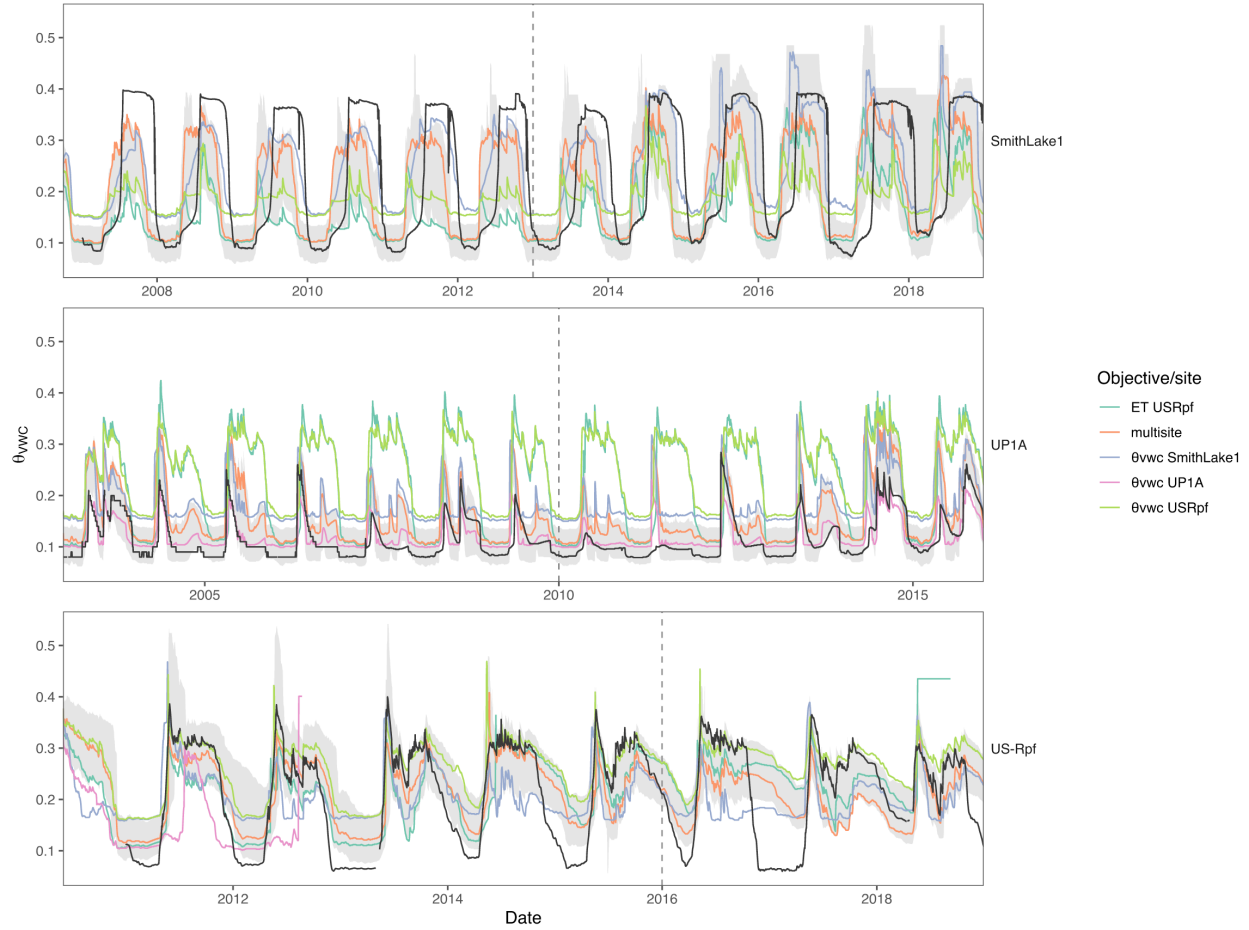
367

368

369 Figure 6. Observed and modeled soil moisture for each site. The black line represents observations at

370 approximate rooting depth at each site, and the colored lines represent multiple selected model parameters

371 based on individual objective functions and a multisite compromise. Gray error bars indicate the range of

372 values simulated by the behavioral parameter sets. Vertical dashed line indicates transition from

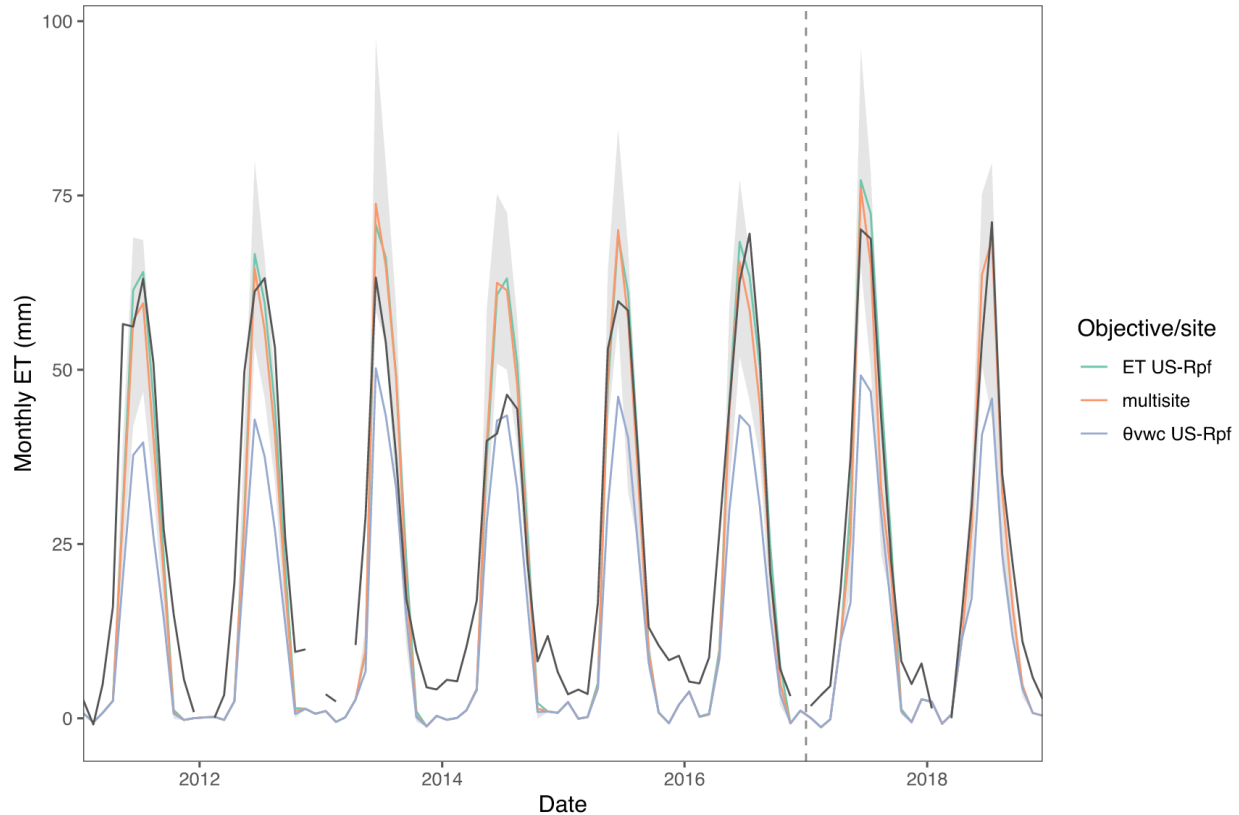373 calibration to validation period.

374

375

376   Figure 7. Observed and modeled monthly ET at US-Rpf, the only site where ET was available. Gray

377   shaded area represents the range of all behavioral parameter sets; black line represents observations, and

378   colored lines represent selected parameter sets as indicated in the legend. Vertical dashed line indicates

379   transition from calibration to validation period.

380

381   3.4 Climate projections and sensitivity

382   Climate projections in bias-corrected, dynamically downscaled NCAR-CCSM4 and GFDL-CM3 indicate

383   increases from 1970-2000 to 2070-2100 in mean annual temperature ranging between sites from 10.3-

384   12.5 °C in GFDL-CM3 and 6.4-7.7 °C in NCAR-CCSM4 (Figure 8). The range of changes in projected

385   precipitation is much greater between GCMs and sites, with projected changes in GFDL-CM3 much

386   greater than those in NCAR-CCSM4. At US-Rpf, projected increase in precipitation was 13.1-36.0%,

387   depending on GCM; projected increase in precipitation was 68-190% at UP1A and 72-396% at Smith

388   Lake 1. This exaggerated large increase in precipitation in GFDL-CM3 at Smith Lake 1 is due in part to

389   the bias-correction: the uncorrected, downscaled data in GFDL-CM3 has 510 mm of precipitation at

390   Smith Lake 1 in 1970-2000, but the bias-corrected data has only 139 mm; in the 2070-2100 period, the

391   downscaled data has 940 mm while the bias-corrected results has 690 mm. The absolute differences are

392   reasonably comparable between the bias-corrected and downscaled data, but the percent differences

393   increase dramatically due to the smaller denominator in the bias-corrected data.
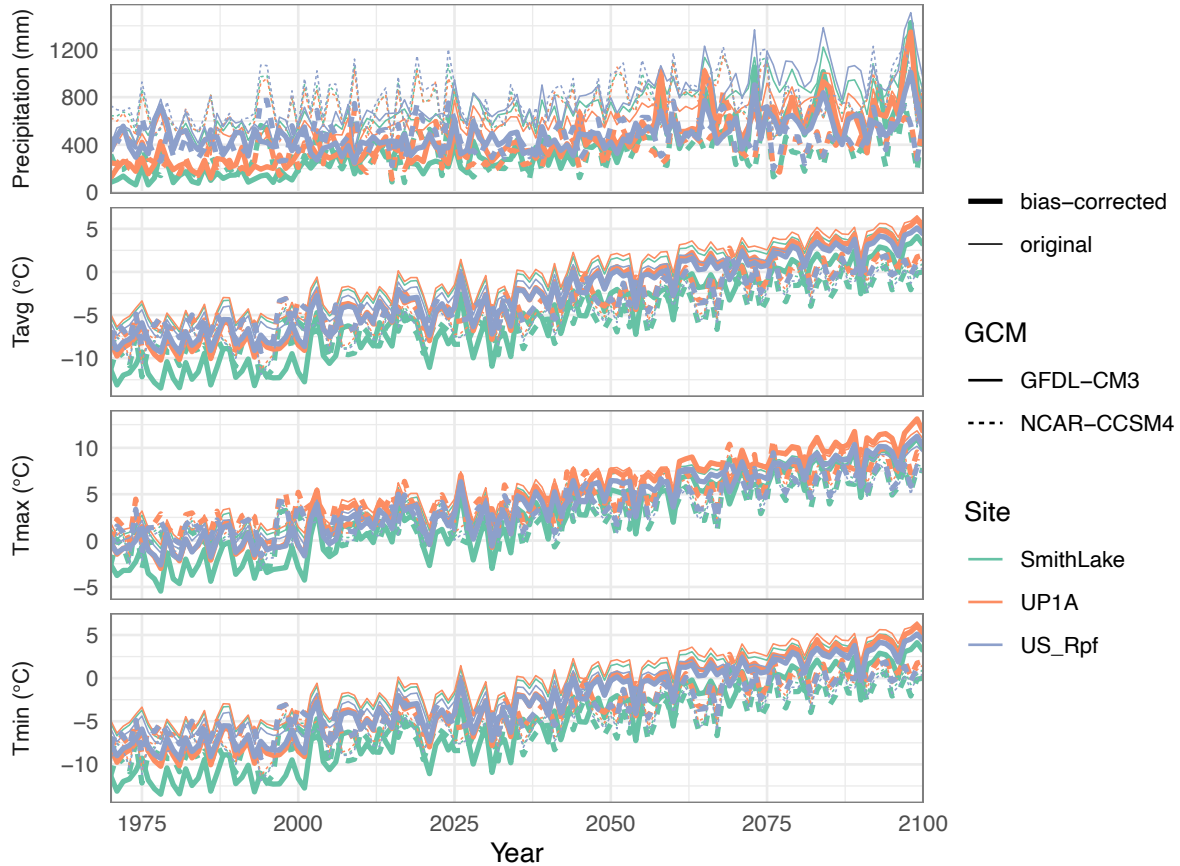
394

395

396   Figure 8. Projections of future climate variables with two GCMs, summarized annually. Thicker lines

397   indicate bias-corrected data, while thin lines show the WRF-downscaled data.

398

399   Choice of parameter set and GCM had comparable effects on trends in growing season θ_{VWC} to the total

400   effect of climate change, though these differences varied considerably between sites (Table 3; Figure 9).

401   At Smith Lake 1, growing season θ_{VWC} was projected to change by an average of $+0.067 \pm 0.211$ cm^3/cm^3

402   in GFDL-CM3 and -0.095 ± 0.157 cm^3/cm^3 in NCAR-CCSM4. In both GCMs, the high standard

403   deviation relative to the mean change suggests that the variability due to parameter selection is greater

404   than the projected impacts of climate change, and that even the sign of the projected change depends on

405   GCM choice and parameter selection. Moreover, the difference between mean results for each GCM

406   (0.162 cm^3/cm^3) is greater than the mean projected impacts of climate change in either GCM, and is of a

407   similar magnitude to the uncertainty due to parameter set selection. At UP1A, the mean projected change

408   in growing season θ_{VWC} was greater than the standard deviation across parameter sets in both GCMs,

24

409   suggesting that the impacts of climate change in this case were greater than those of parameter selection;

410   notably, the mean impacts of climate change in NCAR-CCSM4 were almost zero. GCM choice was also

411   important in this case, with considerable wetting in GFDL-CM3 and almost zero mean change in NCAR-

412   CCSM4. At US-Rpf, the mean effect of climate change was greater than parameter set variability in

413   GFDL-CM3, but not in NCAR-CCSM4. In US-Rpf as in UP1A, the mean changes in growing season

414   θ_{VWC} were close to zero with NCAR-CCSM4 forcing but showed considerable wetting across most

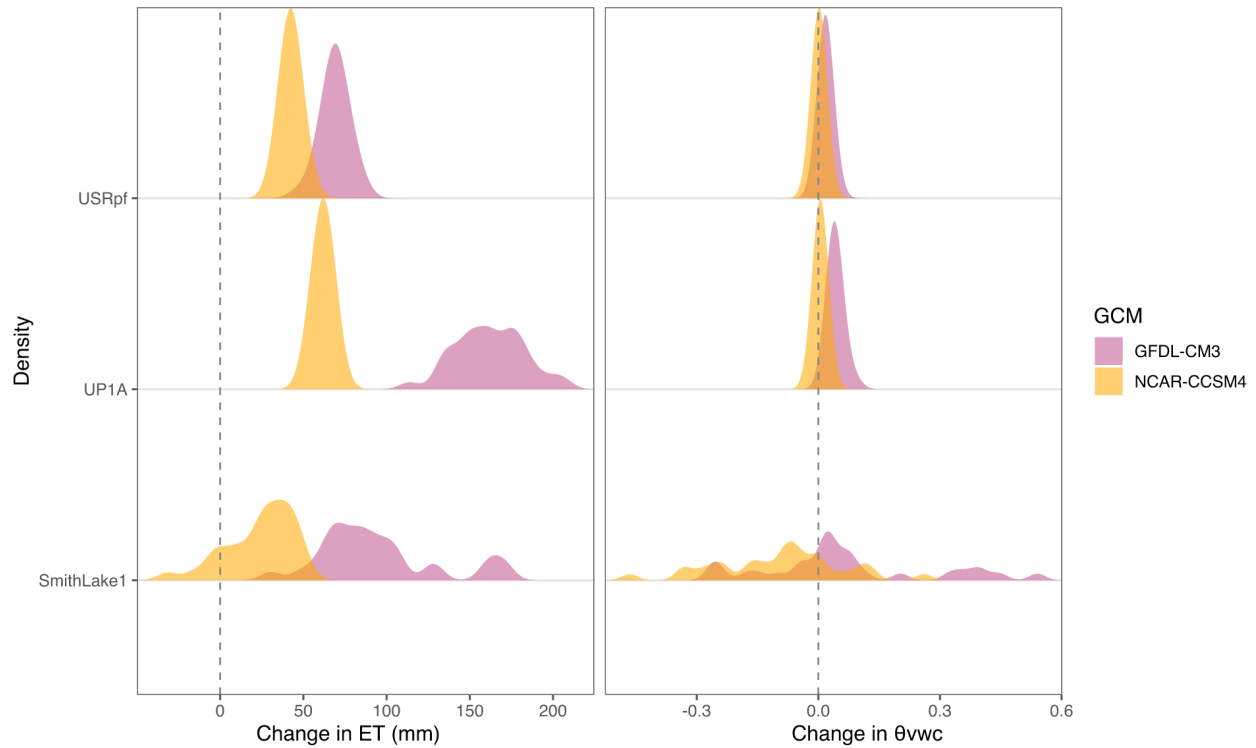415   parameter sets in GFDL-CM3.

416

417

418   Figure 9. Percent change from 1970-2000 to 2070-2100 in growing season ET (left) and mean θ_{VWC} at

419   approximate rooting depth (right) for 35 behavioral parameter sets at each site in two GCMs.

420

421   Table 3. Mean and standard deviations of projected changes in growing season soil moisture and ET
422   between sites and GCMs.

GCM	Site	Change in θ_{VWC} (%)	Change in ET (%)
GFDL-CM3	SmithLake1	0.067 ± 0.211	94 ± 36
NCAR-CCSM4		-0.095 ± 0.157	24 ± 20

GFDL-CM3	UP1A	0.042 ± 0.014	162 ± 21
NCAR-CCSM4		0.005 ± 0.003	62 ± 5
GFDL-CM3	USRpf	0.018 ± 0.006	69 ± 8
NCAR-CCSM4		0.002 ± 0.002	42 ± 5

423

424   Changes in ET were predominantly positive, and the relative effect of parameter sets, GCM, and climate

425   change varied between sites. At Smith Lake 1, the projected change in ET was greater than the standard

426   deviation across parameter sets for both GCMs, though the mean difference between GCMs (70

427   percentage points) was greater than the average projected change in ET by NCAR-CCSM4. At UP1A,

428   change in ET was less dependent on choice of parameter set, but there was a difference of 100 percentage

429   points in the projected mean change between the two GCMs. At US-Rpf, results were more consistent

430   between GCMs and parameter sets: the mean difference in ET increase between the two GCMs was only

431   27 percentage points, and the coefficient of variation across parameter sets was approximately 9 for both

432   GCMs.

433

434   Some parameters contributed more to future wetting or drying trends than others, though relatively few

435   have a statistically significant effect on wetting or drying trends (Figure 10). The only parameter with a

436   statistically significant effect on change in future θ_{VWC} was maximum ponding depth, and it had a

437   statistically significant effect only at USRpf. Higher maximum ponding depth tended to result in reduced

438   θ_{VWC} in the simulations forced with NCAR-CCSM4 (Figure 11). At UP1A, higher θ_{sat} in the first and

439   second layers, and a higher r in the Jarvis-Stewart stomatal conductance functions all had a statistically

440   significant effect on changes in ET, and higher values of these parameters tended to result in higher

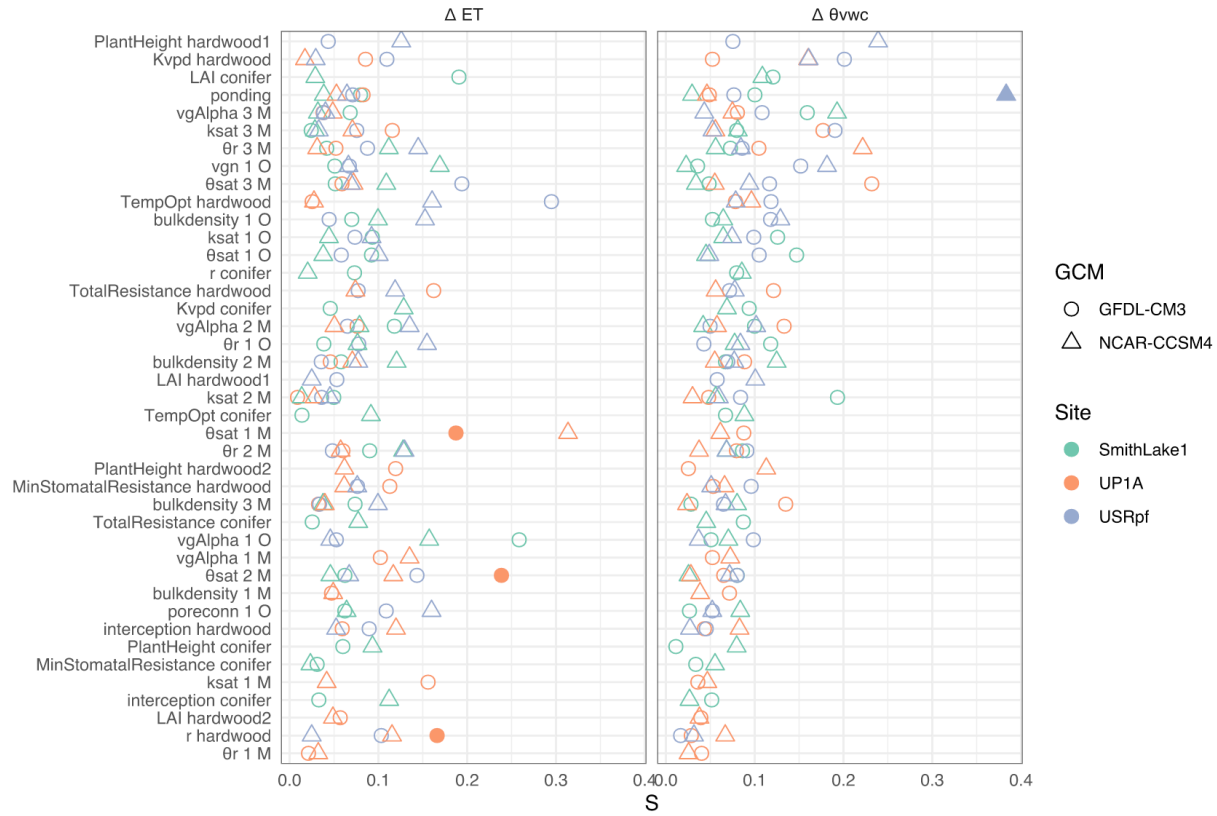441   increases in ET in the simulations forced with GFDL-CM3.

442

443

444 Figure 10. HSIC results showing parameters at each site to which change in ET and change in growing

445 season soil moisture are sensitive. Parameters are ordered based on their mean S across sites and GCMs.

446 The filled points were statistically significant, with p-values indicating that the false discovery rate was

447 less than 0.1 for each site. O = organic; M = mineral and numbers 1-3 indicate soil layer; see Table S1 for

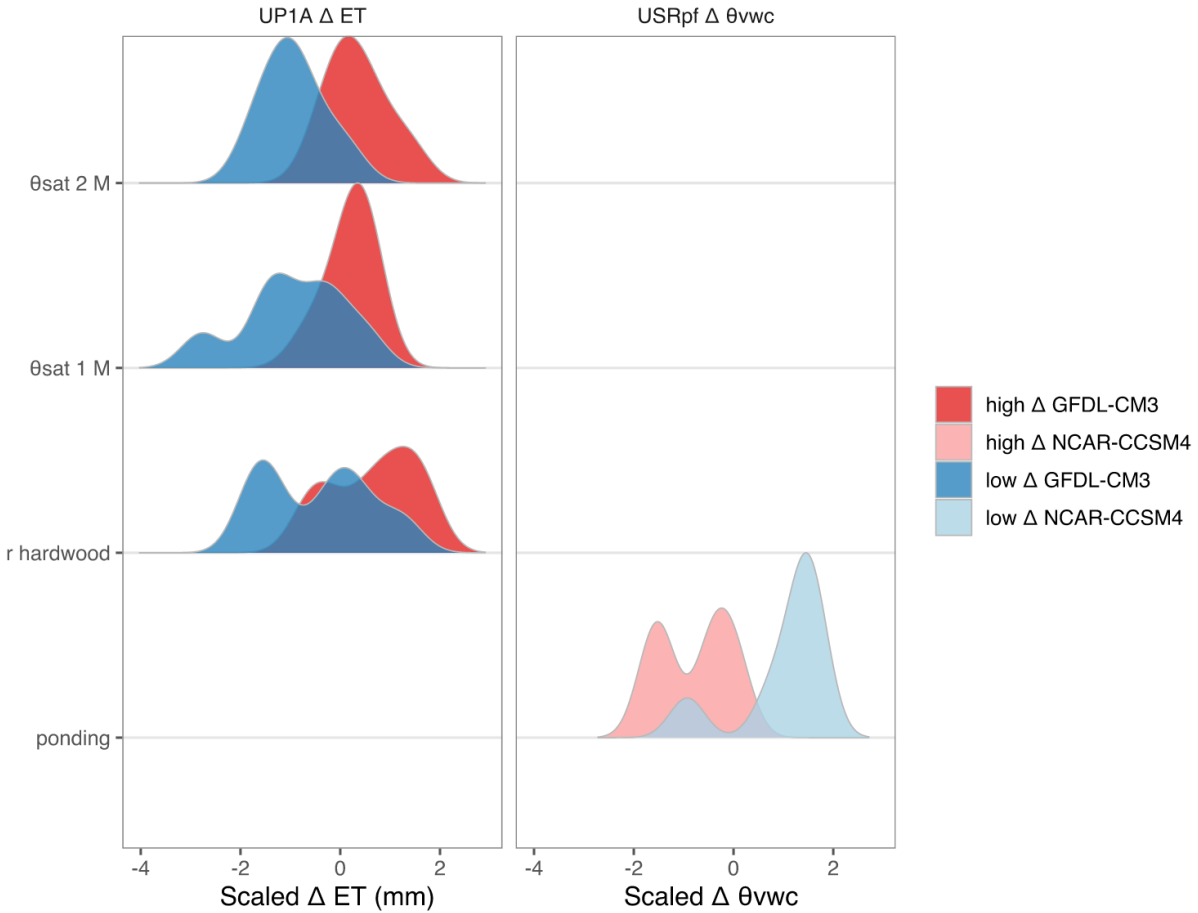448 additional parameter descriptions.

449

450

451

452   Figure 11. Distribution of scaled parameter values that contribute to the results with the largest and

453   smallest 20% of changes in VWC or ET at each site. Only statistically significant parameters are shown;

454   some site/variable combinations had no significant parameters.

4 Discussion

455

456   4.1 Sensitivity analysis

457   At both sites, the most influential inputs were the van Genuchten hydraulic parameters in the soil layer in

458   which soil moisture was evaluated. Soil hydraulic parameters in subjacent layers were also quite sensitive

459   in some cases, though they often had the opposite direction of effect: for example, higher θ_{VWC} in the

460   target layer was associated with higher α in that layer, but lower α in the subjacent layer. This is

461   consistent with the model physics, but may not be immediately obvious during manual calibration. It is

462   also an example of a parameter interaction that should be taken into consideration when interpreting and

463   determining hydrologic model parameters. The sensitivity results also depend to some extent on the width

464   of the prior distributions, which were determined by a detailed literature review. The results should

465   therefore be interpreted with the view that the prior distributions are necessarily somewhat subjective,

466   depending on available literature and modeler interpretation of that literature. Nevertheless, the results of

467   the sensitivity analysis suggest that soil hydraulic parameters throughout the soil profile should be

468   carefully considered in ecohydrological model calibrations.

469

470   4.2 Parameter estimation and uncertainty

471   SHAW was able to simulate soil moisture dynamics reasonably well across multiple sites over 8-13 years.

472   Parameter sets were identified to minimize error at individual sites, but a multisite, multiobjective

473   compromise parameter set also provided acceptable performance. The decline in performance of the

474   compromise parameter set relative to those that performed best at individual sites highlights the risks of

475   overfitting the model to an individual site or objective. Previous comparable modeling studies in boreal

476   regions have found mean error of soil moisture in the rooting zone equal to 0.02, which is lower than the

477   error we generally found when multiple sites were included (Launiainen et al., 2019). Several other soil

478   moisture modeling studies in boreal regions note the difficulty of modeling soil moisture, relative to soil

479   temperature, and provide figures illustrating observed and modeled soil moisture, but lack fit statistics for

480   comparison (Houle et al., 2012; Jones et al., 2014). The relatively poor model performance at Smith Lake

481   2, particularly relative to the other sites, suggests a model structural deficiency. Most likely, this is due to

482   the low slope and topographic position and potential for high net lateral flow at this site given the one

483   dimensional nature of the SHAW model. Recent improvements in SHAW have allowed for the inclusion

484   of subsurface lateral flow, which could facilitate the use of SHAW in lowland regions.

485

486   The results of our GLUE uncertainty analysis indicate that most parameters were not very well

487   constrained relative to the prior distributions, though the parameters that had high sensitivity and were

488   only used at one site (e.g., LAI at each of the hardwood sites) tended to be relatively well constrained by

489   the calibration. This suggests that differences between sites limit parameter identifiability within our

490   modeling context. An alternative to the approach presented here would be to calibrate SHAW against

491   fully spatially distributed data products, whether remotely sensed or interpolated (Zwieback et al., 2019).

492   While this would provide more explicit spatial variability, it also introduces additional errors in the

493   calibration data, which run the risk of contributing disinformative data (Beven & Westerberg, 2011).

494   Future improvements to our method could leverage data from more sites and include more stratification

495   of soils by texture and organic layer class (i.e., live moss vs dead moss). However, this is limited by the

496   availability of sites with high quality climate data inputs and validation data. For instance, in the

497   AmeriFlux site network, which provided important data for this study, there are about twice as many sites

498   per km^2 in the contiguous United States as in Alaska (25 sites per million km^2 in Alaska, and 47 sites per

499   million km^2 in CONUS). In interior Alaska, upland sites with these data characteristics are particularly

500   rare and are more appropriate for the SHAW model than lowland sites with large expected net subsurface

501   lateral flows (Govind et al., 2011).

502

503   Another finding of note was that the parameter set that minimized θ_{VWC} RMSE at US-Rpf tended to

504   underestimate ET at the same site. This may suggest tradeoffs between soil hydraulic and plant hydraulic

505   parameter accuracy. For instance, this parameter set had low LAI and high $r_{s,min}$, which may have reduced

506   plant water use and controlled soil moisture in rooting depth via relatively high van Genuchten α in the

507   adjoining layers. While the wide range of parameter values in the literature makes it difficult to constrain

508   these parameters, multi-objective model calibration can reduce equifinality to some extent, in alignment

509   with previous findings (Efstratiadis & Koutsoyiannis, 2010).

510

511   4.3 Climate projection uncertainty

512   In this study, parameter uncertainty and GCM choice contributed about as much to future soil moisture

513   and ET uncertainty as the total effect of changing climate in the less sensitive GCM, NCAR-CCSM4.

514   This finding reinforces the importance of assessing and reporting sensitivity and uncertainty in

515   environmental simulation models (Saltelli et al., 2019), and, in addition to model structure, may explain

516   some of the spread in projected future soil moisture across multiple hydrologic models when parameter

517   uncertainty is not accounted for (Andresen, 2020). Our finding that parameter uncertainty is quite

518   important contrasts somewhat with previous studies (Dobler et al., 2012; Feng & Beighley, 2020), though

519   these have focused primarily on discharge in temperate regions. This could be because the effects of

520   climate change on soil moisture and ET in boreal Alaska are relatively small compared to projected

521   changes in discharge in temperate regions, or it could suggest that our criteria for behavioral parameter

522   sets are looser than previous studies, though this is difficult to directly assess. These results highlight

523   challenges related to subjectivity in choices of "behavioral" parameter sets, GCMs used as input data, and

524   the climate scenario considered. This inherent subjectivity may be impossible to eradicate from the

525   practice of modeling, but should be recognized and explicitly considered when interpreting model results.

526

527   Finally, our results demonstrate the effects of individual parameters on projected changes in soil moisture

528   and ET. In general, soil moisture in SHAW and similar models can be controlled via soil hydraulic and

529   plant hydraulic parameters, with equifinality in the balance between the two. The parameters that have a

530   statistically significant effect on change in ET and soil moisture vary between sites and objective, but

531   include θ_{sat}, ponding, and the Jarvis-Stewart *r* parameter, which controls the shape of the stomatal

532   conductance response to vapor pressure deficit, with high values resulting in more sensitivity of stomatal

533   conductance to vapor pressure deficit. While the statistical significance of these parameters varies

534   between the GCMs used for forcing and sites, the effect directions are consistent with expectations. For

535   example, high θ_{sat} in the first and second soil layers tended to increase ET. This could be due to the fact

536   that higher water holding capacity can exceed evaporative demand in historical conditions but not in

537   future conditions, leading to large increases in ET. Similarly, higher values of *r* tended to result in greater

538   increases in ET, which is to be expected in energy-limited environments, where ET may be primarily

539   sensitive to vapor pressure deficit. While previous studies have quantified the uncertainty in future

540   climate projections that can result from equifinality (Mendoza et al., 2016), the effect direction of

541   particular parameter choices has not, to our knowledge, been previously assessed quantitatively. Even in

542   contexts in which a full uncertainty analysis is not feasible, we suggest that modelers should explicitly

543   consider and discuss their parameter value selection relative to known ranges of values, and the potential

544   effects of these parameter selections on projected climate change impacts in a given model.

545

5 Conclusions

547   In this study, we conducted a global sensitivity analysis of a process-based hydrologic model at two

548   contrasting boreal sites, providing a screening and ranking of sensitive parameters. Soil hydraulic and

549   plant hydraulic parameters were most sensitive at both sites. We calibrated these sensitive parameters in a

550   GLUE parameter calibration and uncertainty analysis against soil moisture and ET, and identified

551   parameters that were most successful in reasonably reproducing VWC and ET across multiple sites.

552   Critically, we note that the parameter sets identified here should be considered not as an absolute truth,

553   but as a useful set of parameters for modeling in upland boreal forests. Finally, we compared the effect of

554   parameter and GCM selection on changes in soil moisture and ET, finding that these selections can

555   influence the magnitude of projected changes about as much as the total impact of projected climate

556   change, and in some cases, can even influence the sign of projected changes. In a novel contribution, we

557   also identified the parameters to which projected changes in hydrology were most sensitive and the

558   direction of effect of these parameters. While previous studies have assessed the importance of

559   equifinality for climate change impacts assessments, this assessment of the most important parameters

560   and direction of their effects can provide guidance to modellers and consumers of modeling studies who

561   want to understand how specific parameter selections affect estimates of climate change impacts on

562   hydrologic states and fluxes in boreal regions.

Acknowledgments, Samples, and Data

570

571   Data used to develop model inputs are available as cited throughout the methods section. SHAW model

572   inputs and outputs used in this manuscript are published as: Marshall et al. (2021) SHAW model inputs

573   and outputs in boreal Alaska, Hydroshare,

574   https://www.hydroshare.org/resource/5a355d67357a4b8591def61602fe276b/.

575

References

577   Alexander, H. D., Mack, M. C., Goetz, S., Beck, P. S. A., & Belshe, E. F. (2012). Implications of

578   increased deciduous cover on stand structure and aboveground carbon pools of Alaskan boreal

579   forests. *Ecosphere*, *3*(5), art45. https://doi.org/10.1890/ES11-00364.1

580   Anderson, E. A. (1976). *A Point Energy and Mass Balance Model of a Snow Cover*. U.S. Department of

581   Commerce, National Oceanic and Atmospheric Administration, National Weather Service, Office

582   of Hydrology.

583   Andresen, C. G., Lawrence, D. M., Wilson, C. J., McGuire, A. D., Koven, C., Schaefer, K., et al. (2020).

584   Soil moisture and hydrology projections of the permafrost region – a model intercomparison. *The

585   Cryosphere (Online)*, *14*(2). https://doi.org/10.5194/tc-14-445-2020

586   Bartlett, P. A., McCaughey, J. H., Lafleur, P. M., & Verseghy, D. L. (2003). Modelling

587   evapotranspiration at three boreal forest stands using the CLASS: tests of parameterizations for

588   canopy conductance and soil evaporation. *International Journal of Climatology*, *23*(4), 427–451.

589   https://doi.org/10.1002/joc.884

590   Bartsch, A., Balzter, H., & George, C. (2009). The influence of regional surface soil moisture anomalies

591   on forest fires in Siberia observed from satellites. *Environmental Research Letters*, *4*(4), 045021.

592   https://doi.org/10.1088/1748-9326/4/4/045021

593   Beven, K. (2006). A manifesto for the equifinality thesis. *Journal of Hydrology*, *320*(1), 18–36.

594   https://doi.org/10.1016/j.jhydrol.2005.07.007

595   Beven, K., & Binley, A. (1992). The future of distributed models: Model calibration and uncertainty
596   prediction. *Hydrological Processes*, *6*(3), 279–298. https://doi.org/10.1002/hyp.3360060305

597   Beven, K., & Binley, A. (2014). GLUE: 20 years on. *Hydrological Processes*, *28*(24), 5897–5918.
598   https://doi.org/10.1002/hyp.10082

599   Beven, K., & Westerberg, I. (2011). On red herrings and real herrings: disinformation and information in
600   hydrological inference. *Hydrological Processes*, *25*(10), 1676–1680.
601   https://doi.org/10.1002/hyp.7963

602   Bieniek, P. A., Bhatt, U. S., Walsh, J. E., Rupp, T. S., Zhang, J., Krieger, J. R., & Lader, R. (2016).
603   Dynamical Downscaling of ERA-Interim Temperature and Precipitation for Alaska. *Journal of*
604   *Applied Meteorology and Climatology*, *55*(3), 635–654. https://doi.org/10.1175/JAMC-D-15-
605   0153.1

606   Bladon, K. D., Silins, U., Landhäusser, S. M., & Lieffers, V. J. (2006). Differential transpiration by three
607   boreal tree species in response to increased evaporative demand after variable retention
608   harvesting. *Agricultural and Forest Meteorology*, *138*(1–4), 104–119.
609   https://doi.org/10.1016/j.agrformet.2006.03.015

610   Blain, C. A., & Milly, P. C. D. (1991). Development and application of a hillslope hydrologic model.
611   *Advances in Water Resources*, *14*(4), 168–174. https://doi.org/10.1016/0309-1708(91)90012-D

612   Blanken, P. D., Black, T. A., Yang, P. C., Neumann, H. H., Nesic, Z., Staebler, R., et al. (1997). Energy
613   balance and canopy conductance of a boreal aspen forest: Partitioning overstory and understory
614   components. *Journal of Geophysical Research: Atmospheres*, *102*(D24), 28915–28927.
615   https://doi.org/10.1029/97JD00193

616   Bonan, G. B. (1993). Importance of leaf area index and forest type when estimating photosynthesis in
617   boreal forests. *Remote Sensing of Environment*, *43*(3), 303–314. https://doi.org/10.1016/0034-
618   4257(93)90072-6

619   Bonan, G. B., & Sirois, L. (1992). Air temperature, tree growth, and the northern and southern range
620   limits to *Picea mariana*. *Journal of Vegetation Science*, *3*(4), 495–506.
621   https://doi.org/10.2307/3235806

622   Bond-Lamberty, B., Wang, C., Gower, S. T., & Norman, J. (2002). Leaf area dynamics of a boreal black
623   spruce fire chronosequence. *Tree Physiology*, *22*(14), 993–1001.
624   https://doi.org/10.1093/treephys/22.14.993

625   Cable, J. M., Ogle, K., Bolton, W. R., Bentley, L. P., Romanovsky, V., Iwata, H., et al. (2014).
626   Permafrost thaw affects boreal deciduous plant transpiration through increased soil water, deeper
627   thaw, and warmer soils. *Ecohydrology*, *7*(3), 982–997. https://doi.org/10.1002/eco.1423

628 Cahoon, S. M. P., Sullivan, P. F., Brownlee, A. H., Pattison, R. R., Andersen, H.-E., Legner, K., &

629   Hollingsworth, T. N. (2018). Contrasting drivers and trends of coniferous and deciduous tree

630   growth in interior Alaska. *Ecology*. https://doi.org/10.1002/ecy.2223

631 Campbell, G. S., & Norman, J. M. (1998). *An Introduction to Environmental Biophysics*. Retrieved from

632   https://doi.org/10.1007/978-1-4612-1626-1

633 Cannon, A. J. (2016). Multivariate Bias Correction of Climate Model Output: Matching Marginal

634   Distributions and Intervariable Dependence Structure. *Journal of Climate*, *29*(19), 7045–7064.

635   https://doi.org/10.1175/JCLI-D-15-0679.1

636 Carnell, R. (2019). lhs: Latin Hypercube Samples. (Version R package version 1.0.1). Retrieved from

637   https://CRAN.R-project.org/package=lhs

638 Chappell, N. A., Franks, S. W., & Larenus, J. (1998). Multi-scale permeability estimation for a tropical

639   catchment. *Hydrological Processes*, *12*(9), 1507–1523. https://doi.org/10.1002/(SICI)1099-

640   1085(199807)12:9<1507::AID-HYP653>3.0.CO;2-J

641 Chegwidden, O. S., Nijssen, B., Rupp, D. E., Arnold, J. R., Clark, M. P., Hamman, J. J., et al. (2019).

642   How Do Modeling Decisions Affect the Spread Among Hydrologic Climate Change Projections?

643   Exploring a Large Ensemble of Simulations Across a Diversity of Hydroclimates. *Earth's Future*,

644   *7*(6), 623–637. https://doi.org/10.1029/2018EF001047

645 Chen, J. M., Rich, P. M., Gower, S. T., Norman, J. M., & Plummer, S. (1997). Leaf area index of boreal

646   forests: Theory, techniques, and measurements. *Journal of Geophysical Research: Atmospheres*,

647   *102*(D24), 29429–29443. https://doi.org/10.1029/97JD01107

648 Da Veiga, S. (2015). Global sensitivity analysis with dependence measures. *Journal of Statistical*

649   *Computation and Simulation*, *85*(7), 1283–1305. https://doi.org/10.1080/00949655.2014.945932

650 Dang, Q.-L., Margolis, H. A., Coyea, M. R., Sy, M., & Collatz, G. J. (1997). Regulation of branch-level

651   gas exchange of boreal trees: roles of shoot water potential and vapor pressure difference. *Tree*

652   *Physiology*, *17*(8–9), 521–535. https://doi.org/10.1093/treephys/17.8-9.521

653 Dettmann, U., Bechtold, M., Frahm, E., & Tiemeyer, B. (2014). On the applicability of unimodal and

654   bimodal van Genuchten–Mualem based models to peat and other organic soils under evaporation

655   conditions. *Journal of Hydrology*, *515*, 103–115. https://doi.org/10.1016/j.jhydrol.2014.04.047

656 Dobler, C., Hagemann, S., Wilby, R. L., & Stötter, J. (2012). Quantifying different sources of uncertainty

657   in hydrological projections in an Alpine watershed. *Hydrology and Earth System Sciences*,

658   *16*(11), 4343–4360. https://doi.org/10.5194/hess-16-4343-2012

659 Dunn, A. L., Barford, C. C., Wofsy, S. C., Goulden, M. L., & Daube, B. C. (2007). A long-term record of

660   carbon exchange in a boreal black spruce forest: means, responses to interannual variability, and

661   decadal trends. *Global Change Biology*, *13*(3), 577–590. https://doi.org/10.1111/j.1365-

662   2486.2006.01221.x

663 Efstratiadis, A., & Koutsoyiannis, D. (2010). One decade of multi-objective calibration approaches in

664   hydrological modelling: a review. *Hydrological Sciences Journal*, *55*(1), 58–78.

665   https://doi.org/10.1080/02626660903526292

666 Endalamaw, A., Bolton, W. R., Young-Robertson, J. M., Morton, D., Hinzman, L., & Nijssen, B. (2017).

667   Towards improved parameterization of a macroscale hydrologic model in a discontinuous

668   permafrost boreal forest ecosystem. *Hydrol. Earth Syst. Sci.*, *21*(9), 4663–4680.

669   https://doi.org/10.5194/hess-21-4663-2017

670 Feng, D., & Beighley, E. (2020). Identifying uncertainties in hydrologic fluxes and seasonality from

671   hydrologic model components for climate change impact assessments. *Hydrology and Earth*

672   *System Sciences*, *24*(5), 2253–2267. https://doi.org/10.5194/hess-24-2253-2020

673 Flerchinger, G. N. (2017). The Simultaneous Heat and Water (SHAW) Model: Technical Documentation.

674   Technical Report NWRC 2017-02. Retrieved from

675   https://pdfs.semanticscholar.org/4906/2b4ebd161d0df6179b113dd9b1e5abf7813f.pdf

676 Flerchinger, G. N., & Saxton, K. E. (1989). Simultaneous Heat and Water Model of a Freezing Snow-

677   Residue-Soil System 1. Theory and Development. *Transactions of the ASABE*, *32*(2), 565–571.

678 Flerchinger, G. N., Seyfried, M. S., & Hardegree, S. P. (2006). Using Soil Freezing Characteristics to

679   Model Multi-Season Soil Water Dynamics. *Vadose Zone Journal*, *5*(4), 1143–1153.

680   https://doi.org/10.2136/vzj2006.0025

681 Fryer, J. L. (2014). *Picea mariana* (Fire Effects Information System). Online: U.S. Department of

682   Agriculture, Forest Service, Rocky Mountain Research Station, Fire Sciences Laboratory.

683   Retrieved from https://www.fs.fed.us/database/feis/plants/tree/picmar/all.html

684 Goldstein, G. H., Brubaker, L. B., & Hinckley, T. M. (1985). Water relations of white spruce (Picea

685   glauca (Moench) Voss) at tree line in north central Alaska. *Canadian Journal of Forest Research*,

686   *15*(6), 1080–1087. https://doi.org/10.1139/x85-176

687 Govind, A., Chen, J. M., McDonnell, J., Kumari, J., & Sonnentag, O. (2011). Effects of lateral

688   hydrological processes on photosynthesis and evapotranspiration in a boreal ecosystem.

689   *Ecohydrology*, *4*(3), 394–410. https://doi.org/10.1002/eco.141

690 Grayson, R. B., Moore, I. D., & McMahon, T. A. (1992). Physically based hydrologic modeling: 1. A

691   terrain-based model for investigative purposes. *Water Resources Research*, *28*(10), 2639–2658.

692   https://doi.org/10.1029/92WR01258

693   Grossnickle, S. C., & Blake, T. J. (1986). Environmental and physiological control of needle conductance

694   for bare-root black spruce, white spruce, and jack pine seedlings on boreal cutover sites.

695   *Canadian Journal of Botany*, *64*(5), 943–949. https://doi.org/10.1139/b86-126

696   Harp, D. R., Atchley, A. L., Painter, S. L., Coon, E. T., Wilson, C. J., Romanovsky, V. E., & Rowland, J.

697   C. (2016). Effect of soil property uncertainties on permafrost thaw projections: a calibration-

698   constrained analysis. *The Cryosphere*, *10*(1), 341–358. https://doi.org/10.5194/tc-10-341-2016

699   Heijmans, M. M. P. D., Arp, W. J., & Chapin, F. S. (2004). Carbon dioxide and water vapour exchange

700   from understory species in boreal forest. *Agricultural and Forest Meteorology*, *123*(3–4), 135–

701   147. https://doi.org/10.1016/j.agrformet.2003.12.006

702   Helbig, M., Waddington, J. M., Alekseychik, P., Amiro, B. D., Aurela, M., Barr, A. G., et al. (2020).

703   Increasing contribution of peatlands to boreal evapotranspiration in a warming climate. *Nature

704   Climate Change*, *10*(6), 555–560. https://doi.org/10.1038/s41558-020-0763-7

705   Houle, D., Bouffard, A., Duchesne, L., Logan, T., & Harvey, R. (2012). Projections of Future Soil

706   Temperature and Water Content for Three Southern Quebec Forested Sites. *Journal of Climate*,

707   *25*(21), 7690–7701. https://doi.org/10.1175/JCLI-D-11-00440.1

708   Iooss, B., & Lemaître, P. (2015). A Review on Global Sensitivity Analysis Methods. In G. Dellino & C.

709   Meloni (Eds.), *Uncertainty Management in Simulation-Optimization of Complex Systems* (Vol.

710   59, pp. 101–122). Boston, MA: Springer US. https://doi.org/10.1007/978-1-4899-7547-8_5

711   Iooss, B., Veiga, S. D., Janon, A., & Pujol, G. (2020). sensitivity: Global Sensitivity Analysis of Model

712   Outputs (Version R package version 1.22.0). Retrieved from https://CRAN.R-

713   project.org/package=sensitivity

714   Iwata, H., Ueyama, M., Harazono, Y., Tsuyuzaki, S., Kondo, M., & Uchida, M. (2011). Quick Recovery

715   of Carbon Dioxide Exchanges in a Burned Black Spruce Forest in Interior Alaska. *SOLA*, *7*, 105–

716   108. https://doi.org/10.2151/sola.2011-027

717   Iwata, Hiroki, Harazono, Y., & Ueyama, M. (2010). Influence of Source/Sink Distributions on Flux–

718   Gradient Relationships in the Roughness Sublayer Over an Open Forest Canopy Under Unstable

719   Conditions. *Boundary-Layer Meteorology*, *136*(3), 391–405. https://doi.org/10.1007/s10546-010-

720   9513-0

721   Jennings, K. S., Winchell, T. S., Livneh, B., & Molotch, N. P. (2018). Spatial variation of the rain–snow

722   temperature threshold across the Northern Hemisphere. *Nature Communications*, *9*(1), 1148.

723   https://doi.org/10.1038/s41467-018-03629-7

724   Jones, M.-F., Castonguay, M., Nasr, M., Ogilvie, J., Arp, P. A., & Bhatti, J. (2014). Modeling

725   hydrothermal regimes and potential impacts of climate change on permafrost within the South

726   Mackenzie Plain, Northwest Territories, Canada. *Écoscience*, *21*(1), 21–33.

727   https://doi.org/10.2980/21-1-3663

728 Körner, Ch. (1995). Leaf Diffusive Conductances in the Major Vegetation Types of the Globe. In E.-D.

729   Schulze & M. M. Caldwell (Eds.), *Ecophysiology of Photosynthesis* (pp. 463–490). Berlin,

730   Heidelberg: Springer Berlin Heidelberg. https://doi.org/10.1007/978-3-642-79354-7_22

731 Krishnan, P., Black, T. A., Barr, A. G., Grant, N. J., Gaumont-Guay, D., & Nesic, Z. (2008). Factors

732   controlling the interannual variability in the carbon balance of a southern boreal black spruce

733   forest. *Journal of Geophysical Research: Atmospheres*, *113*(D9).

734   https://doi.org/10.1029/2007JD008965

735 Lader, R., Walsh, J. E., Bhatt, U. S., & Bieniek, P. A. (2017). Projections of Twenty-First-Century

736   Climate Extremes for Alaska via Dynamical Downscaling and Quantile Mapping. *Journal of*

737   *Applied Meteorology and Climatology*, *56*(9), 2393–2409. https://doi.org/10.1175/JAMC-D-16-

738   0415.1

739 Lader, R., Walsh, J. E., Bhatt, U. S., & Bieniek, P. A. (2020). Anticipated changes to the snow season in

740   Alaska: Elevation dependency, timing and extremes. *International Journal of Climatology*, *40*(1),

741   169–187. https://doi.org/10.1002/joc.6201

742 Lamhamedi, M., & Bernier, P. (1994). Ecophysiology and field performance of black spruce (Picea

743   mariana): a review. *Annales Des Sciences Forestières*, *51*(6), 529–551.

744   https://doi.org/10.1051/forest:19940601

745 Launiainen, S., Guan, M., Salmivaara, A., & Kieloaho, A.-J. (2019). Modeling boreal forest

746   evapotranspiration and water balance at stand and catchment scales: a spatial approach.

747   *Hydrology and Earth System Sciences*, *23*(8), 3457–3480. https://doi.org/10.5194/hess-23-3457-

748   2019

749 Li, X., Xiao, Q., Niu, J., Dymond, S., McPherson, E. G., van Doorn, N., et al. (2017). Rainfall

750   interception by tree crown and leaf litter: An interactive process. *Hydrological Processes*, *31*(20),

751   3533–3542. https://doi.org/10.1002/hyp.11275

752 Link, T. E., Flerchinger, G. N., Unsworth, M., & Marks, D. (2004). Simulation of Water and Energy

753   Fluxes in an Old-Growth Seasonal Temperate Rain Forest Using the Simultaneous Heat and

754   Water (SHAW) Model. *Journal of Hydrometeorology*, *5*(3), 443–457.

755   https://doi.org/10.1175/1525-7541(2004)005<0443:SOWAEF>2.0.CO;2

756 Liu, H., & Lennartz, B. (2019). Hydraulic properties of peat soils along a bulk density gradient-A meta

757   study. *Hydrological Processes*, *33*(1), 101–114. https://doi.org/10.1002/hyp.13314

758   L.O. Safford, John C. Bjorkbom, & John C. Zasada. (1990). Betula papyifera Marsh. Paper Birch. In
759   *Silvics of North America* (Vol. 2, pp. 158–171). Washington, DC: U.S. Department of
760   Agriculture, Forest Service.

761   Ludwig, R., May, I., Turcotte, R., Vescovi, L., Braun, M., Cyr, J.-F., et al. (2009). The role of
762   hydrological model complexity and uncertainty in climate change impact assessment. *Advances*
763   *in Geosciences*, *21*, 63–71. https://doi.org/10.5194/adgeo-21-63-2009

764   Maire, V., Wright, I. J., Prentice, I. C., Batjes, N. H., Bhaskar, R., van Bodegom, P. M., et al. (2015).
765   Global effects of soil and climate on leaf photosynthetic traits and rates: Effects of soil and
766   climate on photosynthetic traits. *Global Ecology and Biogeography*, *24*(6), 706–717.
767   https://doi.org/10.1111/geb.12296

768   Marshall, A., Link, T., Flerchinger, G., Nicolsky, D., & Lucash, M. (2020). *Ecohydrologic modeling in*
769   *deciduous boreal forest: Model evaluation for application in non-stationary climates* (preprint).
770   Preprints. https://doi.org/10.22541/au.160414217.73787642/v1

771   Melvin, A. M., Mack, M. C., Johnstone, J. F., David McGuire, A., Genet, H., & Schuur, E. A. G. (2015).
772   Differences in Ecosystem Carbon Distribution and Nutrient Cycling Linked to Forest Tree
773   Species Composition in a Mid-Successional Boreal Forest. *Ecosystems*, *18*(8), 1472–1488.
774   https://doi.org/10.1007/s10021-015-9912-7

775   Mendoza, P. A., Clark, M. P., Mizukami, N., Gutmann, E. D., Arnold, J. R., Brekke, L. D., &
776   Rajagopalan, B. (2016). How do hydrologic modeling decisions affect the portrayal of climate
777   change impacts?: Subjective Hydrologic Modelling Decisions in Climate Change Impacts.
778   *Hydrological Processes*, *30*(7), 1071–1095. https://doi.org/10.1002/hyp.10684

779   Menne, M. J., Durre, I., Korzeniewski, B., McNeal, S., Thomas, K., Yin, X., et al. (2012). Global
780   Historical Climatology Network - Daily (GHCN-Daily). *NOAA National Climatic Data Center*,
781   *Version 3*. https://doi.org/10.7289/V5D21VHZ

782   Murray, M., Soh, W. K., Yiotis, C., Spicer, R. A., Lawson, T., & McElwain, J. C. (2020). Consistent
783   Relationship between Field-Measured Stomatal Conductance and Theoretical Maximum Stomatal
784   Conductance in C3 Woody Angiosperms in Four Major Biomes. *International Journal of Plant*
785   *Sciences*, *181*(1), 142–154. https://doi.org/10.1086/706260

786   National Cooperative Soil Survey. (2020). *National Cooperative Soil Survey Soil Characterization*
787   *Database*. Retrieved from http://ncsslabdatamart.sc.egov.usda.gov/

788   Pianosi, F., Beven, K., Freer, J., Hall, J. W., Rougier, J., Stephenson, D. B., & Wagener, T. (2016).
789   Sensitivity analysis of environmental models: A systematic review with practical workflow.
790   *Environmental Modelling & Software*, *79*, 214–232.
791   https://doi.org/10.1016/j.envsoft.2016.02.008

792   Ranney, T. G., & Peet, M. M. (1994). Heat Tolerance of Five Taxa of Birch (Betula): Physiological
793   Responses to Supraoptimal Leaf Temperatures. *Journal of the American Society for Horticultural*
794   *Science*, *119*(2), 243–248. https://doi.org/10.21273/JASHS.119.2.243

795   Salmon, Y., Lintunen, A., Dayet, A., Chan, T., Dewar, R., Vesala, T., & Hölttä, T. (2020). Leaf carbon
796   and water status control stomatal and nonstomatal limitations of photosynthesis in trees. *New*
797   *Phytologist*, *226*(3), 690–703. https://doi.org/10.1111/nph.16436

798   Saltelli, A., Aleksankina, K., Becker, W., Fennell, P., Ferretti, F., Holst, N., et al. (2019). Why so many
799   published sensitivity analyses are false: A systematic review of sensitivity analysis practices.
800   *Environmental Modelling & Software*, *114*, 29–39. https://doi.org/10.1016/j.envsoft.2019.01.012

801   Serbin, S. P., Ahl, D. E., & Gower, S. T. (2013). Spatial and temporal validation of the MODIS LAI and
802   FPAR products across a boreal forest wildfire chronosequence. *Remote Sensing of Environment*,
803   *133*, 71–84. https://doi.org/10.1016/j.rse.2013.01.022

804   Subin, Z. M., Koven, C. D., Riley, W. J., Torn, M. S., Lawrence, D. M., & Swenson, S. C. (2012). Effects
805   of Soil Moisture on the Responses of Soil Temperatures to Climate Change in Cold Regions.
806   *Journal of Climate*, *26*(10), 3139–3158. https://doi.org/10.1175/JCLI-D-12-00305.1

807   Teufel, B., & Sushama, L. (2019). Abrupt changes across the Arctic permafrost region endanger northern
808   development. *Nature Climate Change*, *9*(11), 858–862. https://doi.org/10.1038/s41558-019-0614-
809   6

810   Ueyama, M., Harazono, Y., Kim, Y., & Tanaka, N. (2009). Response of the carbon cycle in sub-arctic
811   black spruce forests to climate change: Reduction of a carbon sink related to the sensitivity of
812   heterotrophic respiration. *Agricultural and Forest Meteorology*, *149*(3), 582–602.
813   https://doi.org/10.1016/j.agrformet.2008.10.011

814   Ueyama, M., Iwata, H., Nagano, H., Tahara, N., Iwama, C., & Harazono, Y. (2019). Carbon dioxide
815   balance in early-successional forests after forest fires in interior Alaska. *Agricultural and Forest*
816   *Meteorology*, *275*, 196–207. https://doi.org/10.1016/j.agrformet.2019.05.020

817   Van Pelt, R. (2007). *Identifying Mature and Old Forests in Western Washington* (p. 104). Olympia, WA:
818   Washington State Department of Natural Resources.

819   Viereck, L. A., Dyrness, C. T., Cleve, K. V., & Foote, M. J. (1983). Vegetation, soils, and forest
820   productivity in selected forest types in interior Alaska. *Canadian Journal of Forest Research*,
821   *13*(5), 703–720. https://doi.org/10.1139/x83-101

822   Wang, J. R., Zhong, A. L., Comeau, P., Tsze, M., & Kimmins, J. P. (1995). Aboveground biomass and
823   nutrient accumulation in an age sequence of aspen (Populus tremuloides) stands in the Boreal
824   White and Black Spruce Zone, British Columbia. *Forest Ecology and Management*, *78*(1), 127–
825   138. https://doi.org/10.1016/0378-1127(95)03590-0

826   Wilby, R. L. (2005). Uncertainty in water resource model parameters used for climate change impact
827   assessment. *Hydrological Processes*, *19*(16), 3201–3219. https://doi.org/10.1002/hyp.5819

828   Wilks, D. S. (2016). "The Stippling Shows Statistically Significant Grid Points": How Research Results
829   are Routinely Overstated and Overinterpreted, and What to Do about It. *Bulletin of the American*
830   *Meteorological Society*, *97*(12), 2263–2273. https://doi.org/10.1175/BAMS-D-15-00267.1

831   Yarie, J., & van Cleve, K. (2010). Long-term monitoring of climatic and nutritional affects on tree growth
832   in interior Alaska. *Canadian Journal of Forest Research. 40: 1325-1335*, *40*, 1325–1335.

833   Yarie, John, & Billings, S. (2002). Carbon balance of the taiga forest within Alaska: Present and future.
834   *Canadian Journal of Forest Research*, *32*, 757–767. https://doi.org/10.1139/x01-075

835   Yarie, John, Kane, E., & Mack, M. (2007). Aboveground Biomass Equations for the Trees of Interior
836   Alaska. *AFES Bulletin*, *115*, 16.

837   Zhang, Y., Carey, S. K., Quinton, W. L., Janowicz, J. R., Pomeroy, J. W., & Flerchinger, G. N. (2010).
838   Comparison of algorithms and parameterisations for infiltration into organic-covered permafrost
839   soils. *Hydrol. Earth Syst. Sci.*, *14*(5), 729–750. https://doi.org/10.5194/hess-14-729-2010

840   Zhang, Y., Cheng, G., Li, X., Han, X., Wang, L., Li, H., et al. (2013). Coupling of a simultaneous heat
841   and water model with a distributed hydrological model and evaluation of the combined model in
842   a cold region watershed. *Hydrological Processes*, *27*(25), 3762–3776.
843   https://doi.org/10.1002/hyp.9514

844   Zwieback, S., Westermann, S., Langer, M., Boike, J., Marsh, P., & Berg, A. (2019). Improving
845   Permafrost Modeling by Assimilating Remotely Sensed Soil Moisture. *Water Resources*
846   *Research*, *55*(3), 1814–1832. https://doi.org/10.1029/2018WR023247

847

848

849